

Cione, J.J., P. Molina, J. Kaplan, and P.G. Black, SST time series directly under tropical cyclones: observations and implications *Proceedings, 24th Conference on Hurricanes and Tropical Meteorology*, pp. 1-2, Boston, MA: American Meteorological Society (2000).

Emanuel, K., Thermodynamic control of hurricane intensity, *Nature*, Vol. 401, pp. 665-669 (1999).

Gentemann, C., D. Smith, and F. Wentz, Microwave SST correlation with cyclone intensity, *Proceedings, 24th Conference on Hurricanes and Tropical Meteorology*, pp. 3-4, Boston, MA: American Meteorological Society (2000).

Ginnis, I., W. Shen, and M. Bender, Performance evaluation of the GFDL coupled hurricane ocean prediction system in the Atlantic basin, *Proceedings, 23rd Conference on Hurricanes and Tropical Meteorology*, pp. 607-610, Boston, MA: American Meteorological Society (1999).

Holland, G.J., and Y. Wang, What limits tropical cyclone intensity, *Preprints of the 23rd Conference on Hurricanes and Tropical Meteorology*, January 10-15, 1999, Dallas, TX pp. 955-958 (1999).

Holland, G.J. and Y. Wang, Limitations on hurricane intensity, *Session 1A of the 24th Conference on Hurricanes and Tropical Meteorology* Fort Lauderdale, FL, Paper 1A.5 (Figure 2-12 of this report provided courtesy of senior author) (2000).

Schade, L.R., and K.A. Emanuel, The ocean's effect on the intensity of tropical cyclones: Results from a simple coupled atmosphere-ocean model, *Journal of the Atmospheric Sciences*, Vol. 56, pp. 642-651 (1999).

The best available copies of the above-identified documents are attached hereto.

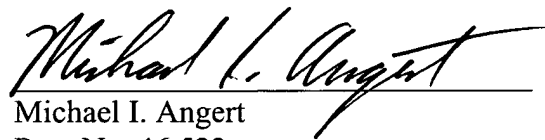
Regarding the 2000 Holland, G.J. and Y. Wang paper, the paper itself is not available. The table of contents of the 24th Conference on Hurricanes and Tropical Meteorology indicating the unavailability of the manuscript is attached. The abstract of the paper was available and is attached hereto. The abstract was downloaded on July 21, 2005 from the following website: <http://ams.confex.com/ams/last2000/24Hurricanes/abstracts/12876.htm>. Figure 2-12 of the paper was available to the Applicants and a color copy of the figure, entitled "Effects of Oceanic Temperature Anomalies" is included for the convenience of the Office.

Any information required to be submitted, that is not attached hereto, is unknown and/or is not readily available to the party or parties from which it was requested.

While Applicants do not believe that any fee is due as a result of this Response, the Office is nevertheless hereby authorized to charge all required fees or credit any overpayments to Deposit Account 11-0600.

If the Examiner believes, for any reason, that personal communication will expedite prosecution of this application, the Examiner is invited to telephone the undersigned at the number provided.

Respectfully submitted,


Michael I. Angert
Reg. No. 46,522

Date: July 26, 2005

Kenyon & Kenyon
1500 K Street, NW, Suite 700
Washington, D.C. 20005-1257
Tel: (202) 220-4393
Fax: (202) 220-4201



Reference No. 1:

Black, P.G., E.W. Ulhorn, J.J. Cione, G.J. Goni, L.K. Shay, S.D. Jacob, E.J. Walsh, and E.A. D'Asaro, Hurricane Intensity Change Modulated By Air-Sea Interaction Effects Based On Unique Interaction Effects Based On Unique Airborne Measurements During The 1998-99 Hurricane Season, *Proceedings, 24th Conference on Hurricanes and Tropical Meteorology*, pp. J7-J8. Boston, MA: American Meteorological Society (2000).

HURRICANE INTENSITY CHANGE MODULATED BY AIR-SEA INTERACTION EFFECTS BASED ON UNIQUE AIRBORNE MEASUREMENTS DURING THE 1998-99 HURRICANE SEASONS

Peter G. Black^{*1}, Eric W. Uhlhorn¹, Joseph J. Cione¹, Gustavo J. Goni², Lynn K. Shay³,
S. Daniel Jacob³, Edward J. Walsh⁴, Eric A. D'Asaro⁵

¹NOAA/AOML- Hurricane Research Division, Miami, Florida

²NOAA/AOML- Physical Oceanography Division, Miami, Florida

³U. of Miami/ RSMAS- Div. of Meteorology and Physical Oceanography, Miami, Florida

⁴NASA-GSFC (NOAA/ETL), Boulder, Colorado

⁵U. of Washington, Applied Physics Laboratory, Seattle, Washington

1. INTRODUCTION

Unique air-sea interaction measurements were made in Hurricanes Bonnie and Danielle in 1998 and Hurricanes Bret, Dennis and Floyd in 1999 which illustrate the ocean's modulation of hurricane intensity change in several interesting ways, i.e. by 1) cessation of intensification due to a storm-induced decrease in SST and ocean heat potential as defined by Leipper and Volgenau (1972), 2) reduction of intensification rate due to cold wake effects from a previous storm and 3) enhancement of intensification rate due to increased ocean heat potential from pre-existing warm ocean eddies. The objective of this study is to better understand properties of the air-sea interface that can lead to changes in atmospheric boundary layer and ocean mixed layer structure, which in turn can lead to inner core intensity change as well as outer wind structure changes. This study will address the first of these cases- Hurricane Bonnie (1998).

2. DISCUSSION- HURRICANE BONNIE (1998) EXPERIMENT

On 24 Aug. 1998 an air-sea interaction experiment was flown into Hurricane Bonnie. The radar structure (Fig. 1) shows a highly asymmetric distribution of precipitation, the result of moderate environmental shear over the system (measured by GPS dropsondes). Two convective cells in the northeast quadrant at a 40 km radius make up the inner eyewall, while the secondary rainband in the northeast quadrant at a radius of about 90 km constitutes the remainder of the precipitation structure, which is stratiform in nature.

Measurements were made of the two-dimensional ocean surface wave spectrum, surface wind speed, wind and thermodynamic profiles in the atmospheric boundary layer and temperature profiles in the ocean mixed layer using, respectively, the Scanning Radar Altimeter, Stepped Frequency Microwave Radiometer (SFMR), GPS dropsondes and Airborne Expendable Bathythermographs (AXBTs). In addition to a background swell component, the SRA measured a primary, storm-induced swell, shown in Fig. 1

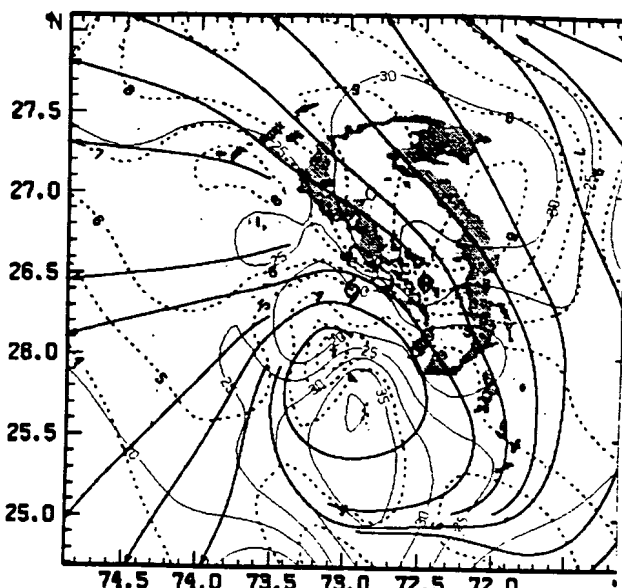


Fig. 1. Radar composite of Hurricane Bonnie with grey shading at 26, 35 and 41 dBZ levels. 'Streamlines' representing primary swell direction from the SRA are overlaid together with contours of swell significant wave height (dashed) and wave steepness (solid).

with a peak significant wave height of 9-10 m in the northeast quadrant extending from 50-150 km radius (just outward from the eyewall and across the principal rainband), and coincident with the surface wind maximum. Fig 1 also shows that the region of growing waves (maximum wave height gradient) is coincident with the region of maximum wave steepness.

Fig. 2 shows that the region of minimum SST (about 26.2C) is located in the southeast quadrant of the storm at a radius of about 150 km from the storm center, or about 2 times the radius of maximum winds (R_{max}). This region is coincident with the region of maximum wave steepness and wave growth shown in Fig. 1. The maximum MLDs are located in the northeast quadrant coincident with the region of maximum swell significant wave height (ranging from 1-2 R_{max}). These observations suggest a strong linkage between the ocean swell field and mixing processes determining MLD deepening rates and rates of mixed layer temperature decrease. We hypothesize that the swell field

^{*}Corresponding author address: Peter G. Black, 4301 Rickenbacker Cswy., Miami, FL 33149; email: black@aoml.noaa.gov

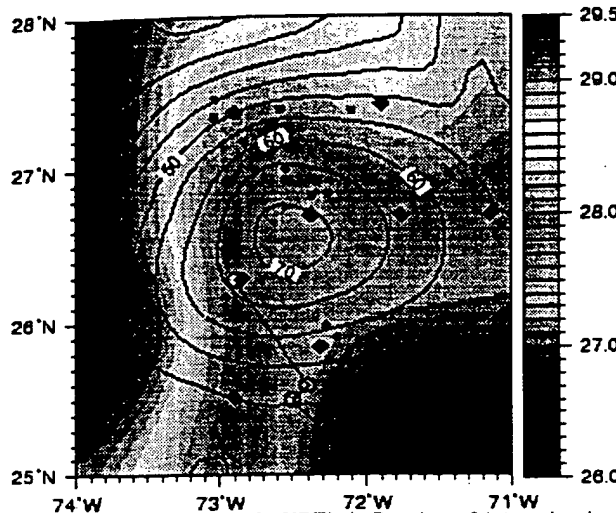


Fig. 2. Objective analysis of AXBT's in Bonnie on 24 Aug showing SST (grey scale on right), mixed layer depth (MLD) in solid contours every 5 m and storm track (solid line with open circles).

may possibly modulate shear processes at the base of the mixed layer and recently measured in Hurricane Dennis (1999) using new 'float' technology (D'Asaro and Black, 2000). Coupled air-sea interactions in Bonnie are discussed further in Cook, et al. (2000). Parameterization of these wave effects on mixing processes, and the resulting changes in surface flux estimates, is a key objective of this research.

3. INTENSITY CHANGE ASSESSMENT

The experiment in Bonnie was conducted 36 hours after cessation of rapid deepening (approximately 1200 UTC, 23 Aug). This corresponded to a change in storm structure from a relatively symmetric, intensely-convective system to an asymmetric, stratiform system (Fig. 1). The time series in Fig. 3 (top panel) indicates a leveling-off of minimum surface pressure (P_{min}), an increase in the outer wind maximum associated with the principal band and a decrease in the inner wind maximum associated with the eyewall during the 36-hour period prior to the experiment. Concurrently, their respective wind radii increased (Fig. 3, middle panel) following a decrease in storm speed to 4 m/s at 1200 UTC, 23 Aug and a resulting SST minimum at 0000 UTC, 24 Aug (Fig. 3, lower panel). We hypothesize that a decrease in the storms' forward motion, induced by environmental ridging north of the storm on the 23rd, resulted in the maximum ocean upwelling zone migrating under the eyewall near R_{max} , enhancing the mixing at the base of the mixed layer, and rapidly cooling the SSTs close to the storm center, which in turn lowered parcel theta-e values, reducing eyewall buoyancy and convective intensity. This weakening of the convection by reduced SSTs appears to have allowed the moderate shear over Bonnie to effect a permanent change in storm structure, resulting in a near steady-state, stratiform system for the ensuing 2 days, until landfall on the 26th.

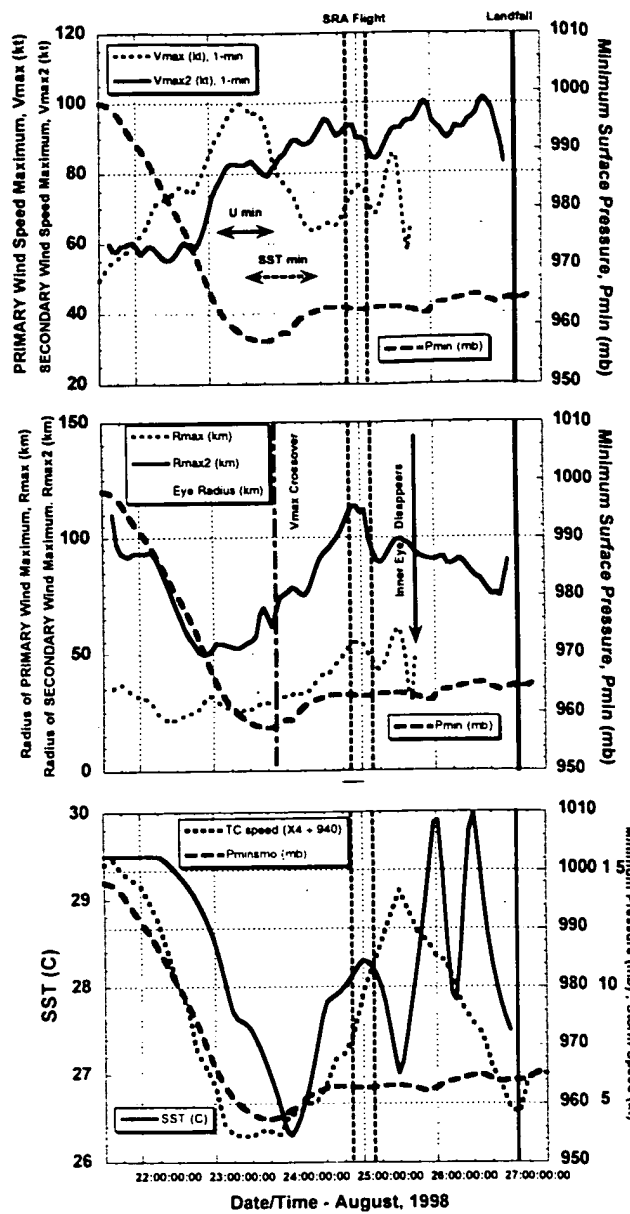


Fig. 3. Time series of intensity and size parameters for Bonnie together with translation speed and SST.

4. REFERENCES

- Cook, T. M., L. K. Shay, P.G. Black, G. J. Goni, M. M. Huber, S. D. Jacob and J. Cione, 2000: Coupled air-sea interactions during Hurricane Bonnie. 24th Conf. On Hurr. and Trop. Meteorol., Ft. Lauderdale, AMS.
- D'Asaro, E. And P. Black, 2000: Turbulence in the ocean boundary layer below Hurricane Dennis. 24th Conf. On Hurr. and Trop. Meteorol., Ft. Lauderdale, AMS.
- Leipper, D. and D. Volgenau, 1972: Hurricane heat potential of the Gulf of Mexico. J. Phys. Oceanogr., 14, 727-746.

Reference No. 2:

Black, P.G., and L.K. Shay, Air-Sea Interaction Processes Relevant To Tropical Cyclone Intensity Change, *Special session on Tropical Cyclone Intensity Change held at the 78th Annual Meeting of the American Meteorological Society* in Phoenix, AZ Paper 4.3 posted: http://www.aoml.noaa.gov/hrd/tcint98/AMS98_4_3.pdf (1999).

AIR-SEA INTERACTION PROCESSES RELEVANT TO TROPICAL CYCLONE INTENSITY CHANGE

Peter G. Black

NOAA/AOML, Hurricane Research Division, Miami, FL 33149

Lynn K. Shay

RSMAS/MPO, University of Miami, Miami, FL 33149

1. INTRODUCTION

It is an important international priority to improve the forecasts of surface windfield, intensity, structure and storm surge in landfalling Tropical Cyclones (TCs) in order to successfully mitigate the detrimental physical impacts associated with these storms. Coastal population growth in the U.S. of 4-5% per year, is outpacing the historic 1-2% per year rate of improvement in official hurricane track predictions. While specific track prediction models have indicated a 15-20% improvement over the past 2-3 years, very little skill has been shown in the prediction of intensity change or windfield distribution (Neumann et al. 1997). For this reason, the average length of coastline warned per storm, about 570 km, has not changed much over the past decade, nor has the average overwarning percentage, about 75%. However, the average preparation costs have increased eight-fold in the past 7 years from \$50M per storm in 1989 (Sheets 1990) to an estimated \$300M per storm in 1996, or about \$1M per mile of coastline warned (Jarrell et al 1992; Neumann et al 1997). The increasing potential for severe loss of life as coastal populations soar, and potential monetary losses of tens of billions of dollars requires that greater effort be directed to understanding all physical processes which play an important role in modulating hurricane windfields and storm surge at landfall.

A major source of difficulty in past efforts to predict hurricane intensity, windfields and storm surge at landfall has been the inability to measure the surface windfield directly and the inability to predict how it changes in response to external and internal forcing. The surface windfield must presently be estimated from a synthesis of scattered surface ship and/or buoy observations and aircraft measurements at 1.5 km to 3.0 km altitude (Powell 1980; Powell et al. 1996; Powell and Houston 1996). This task is complicated by variations with height of the storm's structure, such as the change with height of storm-relative flow due to environmental wind shear and to the variable outward tilt of the wind maximum with height.

2. BACKGROUND

We suggest that changes in the TC intensity and windfield will be brought about by (1) changes in the large-scale environmental conditions, (2) changes in the underlying boundary and/or (3) naturally-evolving internal dynamics. In this paper, we focus discussion on 2) above. One factor affecting hurricanes at landfall is the impact of upper ocean features offshore from the U.S. coastline and the degree to which they modulate TC-

induced cooling of the upper ocean mixed layer. Direct linkages between TC intensity change and observed air-sea changes have been difficult to make due to the multiplicity of factors, above. In addition, detailed oceanographic and surrounding environmental observations in the atmosphere have been generally lacking from which to make comparisons. Innovative use of new observing technologies, mixing mobile observing in-situ platforms, such as drifting buoy arrays and airborne instrumentation, with new satellite observing platforms, are enabling critical features of air-sea and environmental interactions to be measured for the first time.

As TCs approach the U. S. mainland they often encounter warm ocean features such as the Gulf Stream, Florida Current, Gulf Loop Current and Gulf of Mexico warm eddies. Several cases suggesting a strong role of air-sea interaction processes on TC intensity changes have occurred in recent years, many of which have been landfalling situations. One especially significant case was Hurricane Andrew (1992), which gained strength as it passed over the Gulf Stream just before landfall on South Florida (Willoughby and Black, 1996).

Elsewhere in this volume, Shay, et al (1998) describe an innovative use of basin-wide climatology and TOPEX/Poseidon satellite measurements of geoid anomalies to observe these features, which are deep reservoirs of heat and moisture available to significantly intensify landfalling TCs, such as appeared to occur in Hurricane Opal (1995). Cold oceanic features along the shelf zone may also be encountered by TCs just before landfall which may act as an energy sink and weaken the storms just before landfall. Xie et al(1998) make innovative use of NOAA polar orbiting AVHRR satellite imagery to observe this situation in the case of Hurricane Fran, 1996.

The interpretation of a TC's intensity change as it approaches landfall is frequently complicated by trough interaction and oceanic structure change occurring simultaneously. Elsewhere in this volume, Bosart, et al (1998) describe an innovative use of GOES-8 high density water vapor winds to observe an approaching trough interact with Hurricane Opal.

3. THE RECORD HURRICANE SEASONS OF 1995-96

In over half of the 32 storms that occurred during the 1995 and 1996 hurricane seasons, significant intensity changes were associated with storm translation over SST boundaries, which were either pre-existing or created by previous storms. Many of these storms also experienced interactions with mid-latitude troughs during the same time period and has made it difficult to partition the physical processes responsible for the observed intensity changes. This section seeks

Corresponding Author: Peter G. Black, NOAA/AOML, Hurricane Research Division, Miami, FL 33149
Email: black@aoml.noaa.gov

to suggest a link, in selected storms, between changes in air-sea interaction processes and observed intensity changes.

In order to obtain some insight into this process, 10 cases were identified as 1) undergoing significant changes in air-sea fluxes due to changes in the SST field over which they moved and 2) having observations available to document a) the intensity change and b) the SST change. In 1995, these were Felix, Luis, Marilyn, Opal and Roxanne. In 1996, these were Bertha, Edouard, Hortense, Fran and Josephine.

Mobile drifting buoy arrays, provided by the National Data Buoy Center (NDBC) and described in The National Drifting Buoy Deployment Plan (Office of the Federal Coordinator, Silver Spring, MD), were deployed to adaptively sample 3 of these cases of suspected strong ocean interaction: Luis and Marilyn in 1995 and Fran in 1996. An array of 3 Wind Speed/ Direction (WSD) buoys and 7 CMOD mini-drifting buoys were deployed by WC-130 Air Force Reserve (AFRES) aircraft 550 km ahead of Hurricane Luis. The deployment was repeated in the same area for Marilyn 10 days later where a mix of 3 WSD's and 8 CMOD's were deployed. An additional deployment of 35 AXBT's and 3 CMOD's was conducted from a NOAA WP-3D as Marilyn passed over the pre-storm array, providing an unprecedented array of 16 working buoy platforms from which detailed surface wind, pressure, SST and ocean mixed layer depth fields were constructed. The buoy data, together with AVHRR images and FNMOC SST anomaly charts, showed a 4°C decrease in SST's, resulting from Luis, which itself subsequently weakened as it uncovered the cold wake left by Felix one week earlier. Marilyn subsequently crossed Luis' wake at the time convection and attendant surface winds weakened, while at the same time, further enhancing the SST cooling created by Luis and Felix.

In 1995, two storms became quasi-stationary for several days: Felix, offshore from the Gulf Stream, and Roxanne, in the Bay of Campeche. Felix and Roxanne executed slow loops in their respective regions over several days generating SST changes on the order of 3-4°C. This created deep, cold SST pools due to sustained intense upward mixing of subsurface water. Both storms subsequently weakened as convective cloud development declined dramatically.

In 1996, 3 WSD's were deployed 300 km ahead of Fran, just seaward of the Gulf Stream, and adjacent to an offshore NDBC moored buoy. Together these data provided enhanced surface wind and pressure fields. Together with AVHRR images, these data also showed that Fran created a well-defined 2°C cold wake which was interrupted by passage over the Gulf Stream. Fran deepened after emerging from the cold wake created by Edouard five days earlier and then weakened as it approached the warm Gulf Stream. This corresponded to the advection toward the storm's inner core of cool, dry air, associated with a deep mid-latitude trough. In addition, winds ahead of the storm uncovered and amplified a cold shelf eddy on the shoreward side of the 'Charleston Bump' (Xie et al., 1998). A 5°C SST decrease resulted there which may have also played a role in the storm's weakening. This behavior contrasted markedly with the behavior of Hurricanes Andrew

(1992), Jerry (1995) and Bertha (1996), which all intensified just before landfall as they moved over the Gulf Stream.

Also in 1996, Hortense deepened after crossing the cold wake left by Fran ten days earlier. Hortense crossed then paralleled the wake left by Edouard two weeks earlier. After uncovering the cold water in the wake just below the surface, Hortense weakened.

It is our conviction that complex air-sea interactions such as those that occurred during the 1995 and 1996 seasons need to be better understood through improved observational efforts if the hurricane intensity change problem is ever to be understood. Better observations are required of pre-existing ocean feature structure, ocean response to hurricanes, subsequent cold wake evolution and impact on following storms and air-sea flux processes in the hurricane boundary layer. A first step in this direction was taken during the 1997 season in Hurricanes Guillermo (EPAC) and Erika (Atlantic) where new GPS dropsondes were first deployed in quantity within the storms' inner core and subsequently deployed in conjunction with AXBT's. In this way, both atmospheric and oceanic boundary/mixed layer structure were simultaneously measured.

4. HURRICANE OPAL

Hurricane Opal represented the classic dilemma to forecasters in attempting to assess TC intensity change. An upper trough was approaching Opal as it entered the warm Gulf of Mexico. This is illustrated schematically in Fig. 1. The question was how would the trough effect intensity change and how would air-sea interaction effects modulate this interaction. Even in hindsight, this is a difficult question to answer.

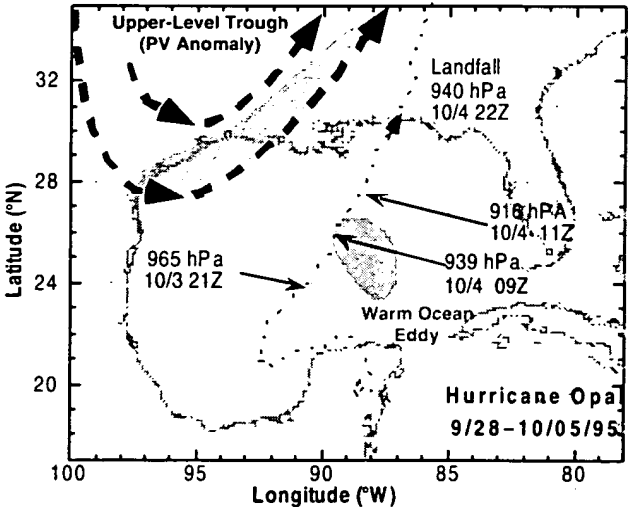


Figure 1. Schematic showing upper trough and jetstreak positions (dashed streamlines and elongated shading, respectively) relative to Opal about 1200 GMT, 3 October, 1995. Opal's track (dotted line) and approximate eddy location (oval-shaped shading) based on Topex/Poseidon are also shown.

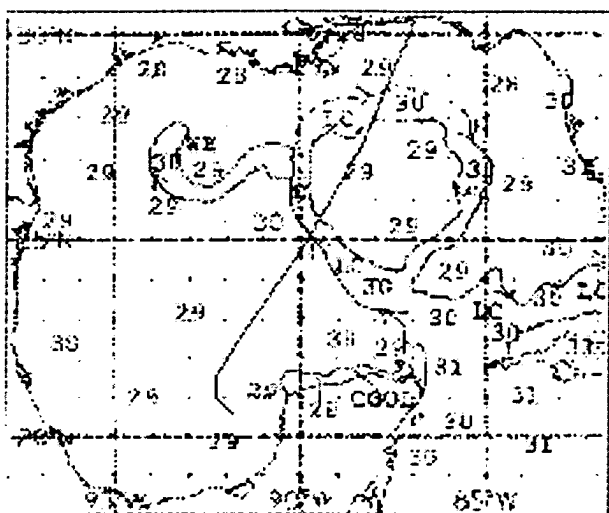


Figure 2. Ocean feature analysis for 26 September, 1995 showing spot SST values ($^{\circ}$ C) and Loop Current/eddy complex in central Gulf.

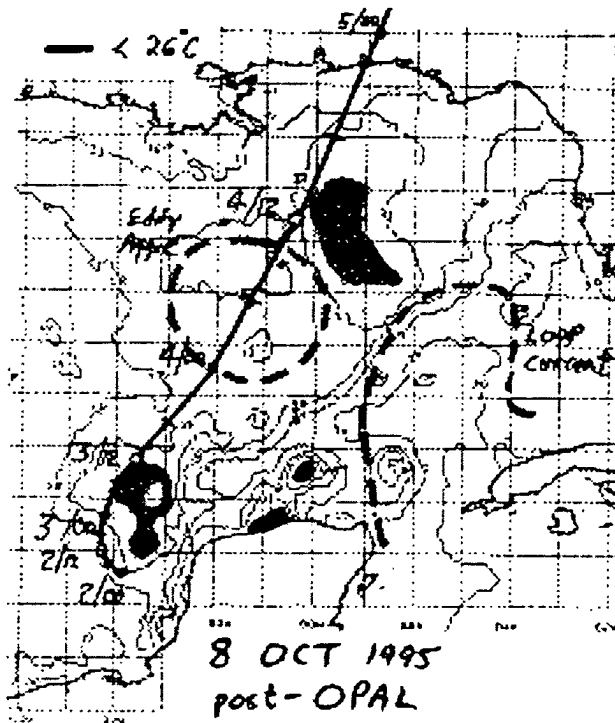


Figure 3. SST analysis ($^{\circ}$ C) for 8 October, 1995. Shading is for SST<26°C. Dashed lines show estimated Loop Current and Eddy Aggie locations. Solid line is Opal's track with closed circles for 00 GMT positions, open circles for 12 GMT locations and tics for 6-hourly positions.

However, Bosart, et al (1998) produce a convincing argument, using high-density water vapor winds to analyze the details of the upper troposphere interaction, to show that a jet streak associated with the trough produced and enhancement of the divergence over the storm just before rapid deepening commenced near 1800 GMT, 3 October. The work of Shay, et al (1998)

show that just after this time, the storm passed over a warm Gulf of Mexico eddy, dubbed "Eddy Aggie" by oceanographers. Using sea surface height anomalies from TOPEX/Poseidon measurements and an innovative new technique to infer mixed layer depth, they calculate the change in ocean mixed layer heat potential. Their results show a large change in mixed layer heat content and contend that the fluxes into Opal had to be enhanced during its passage over the eddy.

This feature was well known to oceanographers, who had been following its pinching-off process from the Loop Current since late Spring using the TOPEX data and AVHRR polar-orbiting satellite data. But the feature was largely unknown to hurricane forecasters since it did not appear in summertime SST analyses. Only in an ocean feature analysis (courtesy Jennifer Clark, formerly NESDIS), was the LOOP Current/Eddy Aggie complex discerned prior to Opal's passage over the Gulf. Shown in Fig. 2, this analysis represents features faintly visible in AVHRR images from 26 September, one week prior to Opal's passage over the eddy. This product was discontinued by NOAA at the end of September.

An SST analysis performed at NHC (courtesy Mike Hopkins) on October 8, 4 days after Opal's eddy passage, shows (Fig. 3) the pattern of cooling caused by the storm off the Yucatan coast, southwest of the eddy and around the northeast perimeter of the eddy. The Loop Current and eddy locations in Fig 3 were estimated from a combination of the TOPEX data and an interpolation between Fig. 2 and the first images of the eddy/Loop Current complex in late November (Fig. 4). Note, from the analysis that no significant surface cooling occurred in the area of the eddy. Yet, the analysis of Shay et al (1998) show that a large change in the ocean upper layer heat content took place. Therefore, large fluxes of heat and moisture had to occur as the storm passed over this eddy. This evidence shows that a deep reservoir of warm ocean water can supply almost infinite amounts of heat energy without themselves being depleted.

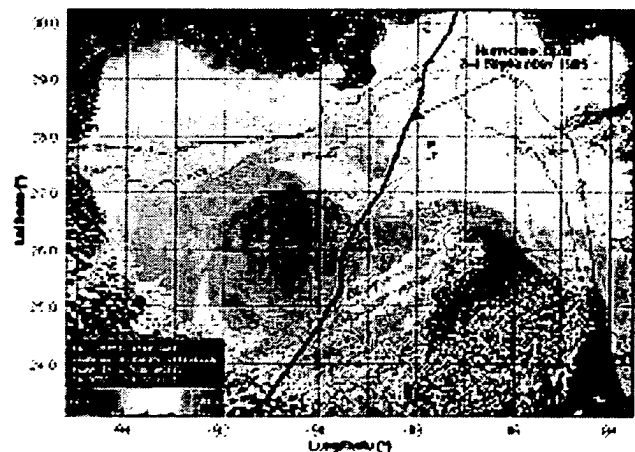


Figure 4. AVHRR image of Eddy Aggie courtesy of LSU Coastal Studies Institute, Earth Scan Laboratory for 26 November, 1995. Opal's position at 3-h intervals are shown by open circles.

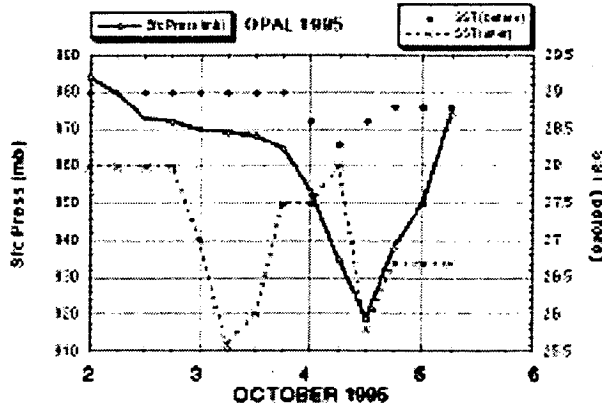


Figure 5. Time series of minimum surface pressure, together with SST along Opal's track before (September 26) and after (October 8) storm passage.

Fig 5 together with Fig 3 show that the storm center moves into the eddy just after rapid deepening has commenced, most likely triggered by the enhanced trough-induced upper divergence. By 1200 GMT, 4 October, the trough-enhanced divergence is gone, but the rapid deepening still continues because of the enhanced surface fluxes over the eddy. The fluxes are immediately cut off as the storm exits the eddy by 1200 GMT, 4 October and moves into the storm-cooled water. Convection quickly dies out and rapid filling commences.

One is tempted to conclude, that given the proper observations, this type of intensity change scenario could be diagnosed ahead of time. However, one other factor to be noted based on analysis of SSM/I 85-GHz images, is that a concentric eyewall cycle was occurring, apparently triggered by the trough interaction (Willoughby and Black, 1996; Willoughby et al 1982) such that the inner eye had shrunk to the point of dissipation by 1300 GMT, 4 October, just as the cold water effect might have resulted in filling. Perhaps the cold SSTs prevented a further contraction of the outer concentric ring of convection and limited any subsequent deepening prior to landfall. Certainly, the issue of the relative role on intensity change of trough interaction, air-sea interaction and internal dynamics deserves considerable further research through enhanced observational efforts.

5. HURRICANE COLD WAKE PRODUCTION AND STORM ASYMMETRIC STRUCTURE

The extent and magnitude of the cold SST region produced by hurricanes has been shown (Black, 1983; Black and Shay, 1995) to be a crescent-shaped region with maximum SST decrease located in the right-rear quadrant. Maximum cooling ranges from 1.5-6°C, depending on the speed of motion of the storm and the underlying mixed layer structure. The radial extent of maximum cooling was shown to range from the radius of maximum winds outward to 2.5 times the radius of maximum winds (R_{max}). The pattern is a consequence and mixing, upwelling and horizontal advection, with strongest cooling in the right-rear quadrant a consequence of combined upwelling and mixing

processes. Beyond 2.5 R_{max} , the pattern is modulated by internal inertia-gravity waves. These conclusions were based on hundreds of AXBT observations in dozens of storms over a 20-year period from 1971 to 1991.

Of relevance to the present discussion is the inference that the cooling pattern can be strongly modulated by pre-existing oceanic features. The extent of this modulation depends on the oceanic structure of the feature and the speed of the storm.

In the case of Opal's passage over Eddy Aggie and the Loop Current, its forward speed accelerated from nearly stationary on 2 October to over 10 m s^{-1} by landfall on 4 October. The effect of the eddy on the storm and vice versa can be quite different for slow moving storms passing over the center of the eddy and for storms passing to the left and right of the eddy.

A summary of these differences is shown in Fig. 6, based on case studies in Black (1983) and in Shay, et al., 1992 for Hurricanes Anita (1976), Allen (1980) and Gilbert (1988). This schematic (Panel A, Fig 6) shows that a slow moving storm may in fact extract all of the available heat potential above 26°C from the mixed layer within an eddy and through the upwelling process bring cold sub-thermocline water to the surface, weakening the eddy circulation by also weakening subsurface horizontal temperature gradients at the edge of the eddy, as was the case for Hurricane Anita. A faster moving storm (panel B), such as Opal, may not be able to cool the eddy at all, but simply extracts enhanced heat and moisture from the eddy, while cooling the perimeter of the eddy dominated by shallower mixed layers.

However, a storm moving near average speeds of 5 m s^{-1} passing to the left of a warm eddy (Panel C) may generate strong cooling along the eddy boundary as a result of complex interactions of storm-generated currents and the eddy currents acting in opposite directions. Such a case was observed for Hurricane Allen and later documented in Hurricane Gilbert with AXCPs (Shay, et al 1992). Finally, a storm moving to the right of a warm eddy (Panel D) may generate only weak cooling at the eddy periphery.

Therefore, a range of possible effects on storm intensity may result from passage over a pre-existing warm eddy such as Eddy Aggie in the Opal case. The fact that it moved rapidly over the center of the eddy suggested that while cooling of the eddy perimeter took place due to strong mixing, that the deeper mixed layers and shorter period of strong mixing allowed Opal to extract energy from the eddy without changing its structure, as shown by Shay, et al (1998). However, other cases such as Anita, Allen and Gilbert produced different scenarios.

Given the four different possible ocean response scenarios discussed above, another factor affecting storm intensity is how the atmospheric PBL asymmetric structure is arranged. Historically, one is lead to expect the strongest convection and highest surface winds to be located in the right-front quadrant of the storm, with maximum inflow and vertical motion in the right-rear quadrant. Aircraft observations over the last 20 years have shown that this is not always the case. Detailed

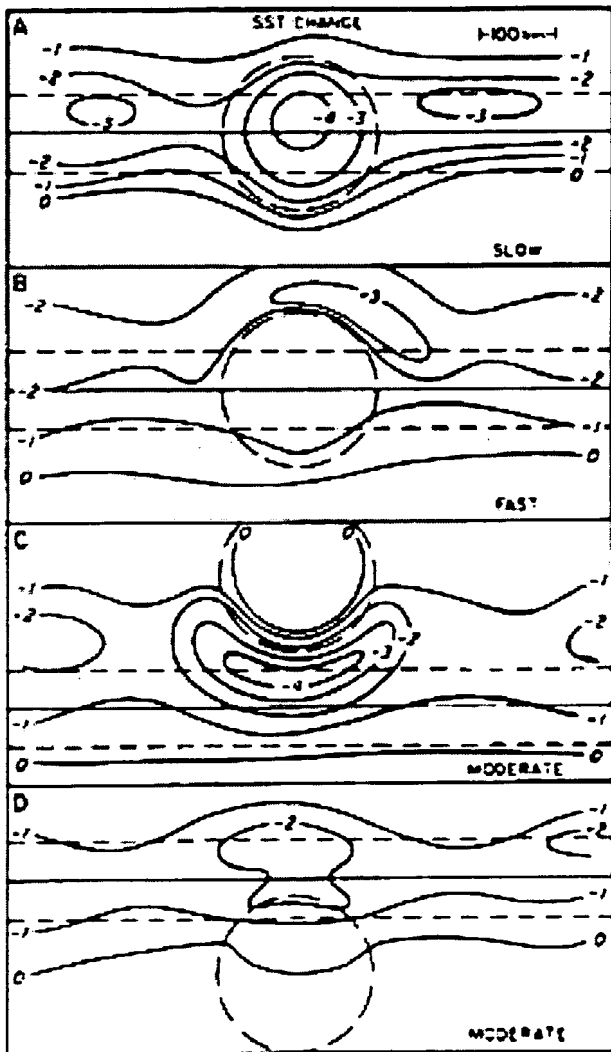


Figure 6. Schematic of SST change ($^{\circ}\text{C}$) induced by a tropical cyclone moving across an oceanic warm eddy for a) fast-moving storm, $U > 7 \text{ m s}^{-1}$, b) slow moving storm, $U < 3 \text{ m s}^{-1}$, c) moderate-moving storm, $3 < U < 7 \text{ m s}^{-1}$, moving to the left of the eddy and d) moderate-moving storm, $3 < U < 7 \text{ m s}^{-1}$, moving to the right of the eddy. Parallel dashed lines are the radius of maximum wind. Circular dashed line in the eddy perimeter.

airborne Doppler radar studies have shown that variations in the environmental vertical shear may cause considerable variability of the location of the strongest convection, maximum winds and quadrant of strongest inflow and vertical motion.

For instance, along track shear such as observed in Hurricanes Norbert (1984) in the eastern Pacific, Celia (1973) in the Gulf of Mexico and Emily (1994) off the North Carolina coast, produce surface wind maxima in the left quadrant of the storm with maximum inflow and vertical motion in the left-front quadrant. These variations can lead the inflowing air to acquire different properties due to fluxes from the surface. If the inflowing air to the eyewall first passes over the cold wake produced by the storm, it may not be sufficiently buoyant to support eyewall convection. If, on the other

hand, the strongest inflowing air at the surface bypasses the cold wake and travels unaffected all the way to the eyewall, much more vigorous inner core convection might be expected.

The capability to measure the storm scale asymmetries and the environmental vertical wind shear may thus play an important role in understanding intensity changes due to air-sea interaction processes. Such a capability is now at hand with the advent of the NOAA G-IVSP aircraft. With the advent of the aerosonde program (Greg Holland, personal communication), this capability may soon exist operationally on a world-wide basis.

6. AIR-SEA TEMPERATURE DIFFERENCES AND HIGH WIND BOUNDARY LAYER STRUCTURE

Yet another wrinkle in the understanding of tropical cyclone (TC) intensity change due to air-sea interaction processes is the recent observations from moored buoys during the passage of TCs. This topic is also discussed in Cione and Black, 1998. Observations first discussed by Black, Holland and Pudov (1993) from moored NDBC buoys in the Gulf of Mexico and the U.S. East Coast and from an oceanographic research ship in the South China Sea showed that the sea minus air temperature difference as a function of wind speed in TC's was not a constant 1°C or less, as historically accepted, but increased to as much as 5°C for winds above hurricane force, i.e. 32 m s^{-1} . This implies that adiabatic cooling which occurs as surface air parcels spiral inward toward lower pressure in the hurricanes' inner core is not balanced by heat flux from the sea, as previously thought.

Holland (1997) has indicated that these results may raise estimates of the Maximum Potential Intensity (MPI) for tropical cyclones by as much as 40 mb for strong storms with estimated MPI of 890 mb. Gray (1995) has indicated that the lower theta-e values implied by a 4°C sea minus air temperature difference and assumptions of relative humidities near 90 %, is in agreement with theta-e values calculated from the Shea and Gray aircraft radial leg data set. This leads to the conclusion of higher MPI values than previously estimated, in agreement with Holland (1997).

Additional observations concerning this issue from two new data sources are now available. The previously reported moored NDBC buoy measurements during hurricane passage in the Gulf of Mexico and off the Atlantic U. S. East Coast south of the Gulf Stream are shown in Fig 1 together with a best fit polynomial regression curve. As mentioned, these results have confirmed earlier measurements made in two typhoons by Pudov (Pudov and Petrichenko, 1988; Korolev, et al., 1990; Pudov and Holland, 1997) from research ships in the South China sea.

In Hurricane Erika (1997) GPS dropsondes were dropped for the first time concurrently with AXBTs, enabling direct measurements of 10-m level air-sea temperature differences to be measured in the hurricane inner core and eyewall region independently of a buoy platform. These points are plotted on Fig. 7 and show excellent agreement with the buoy data.

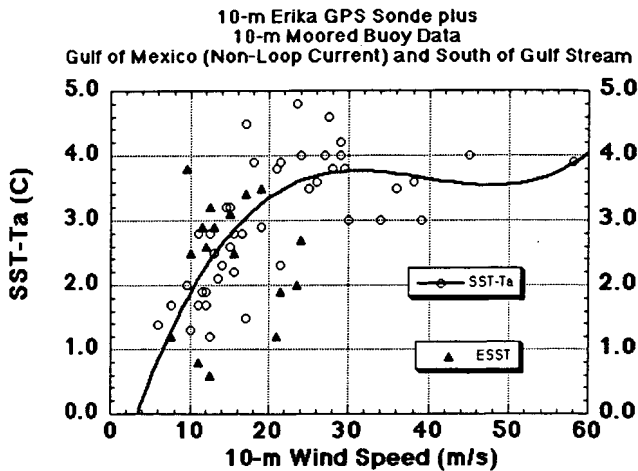


Fig. 7. Scatter plot and regression curve for moored buoy observations at the 10-m level in hurricanes in the Gulf of Mexico outside the deep, warm Loop Current and from buoys off the U. S. East Coast south of the Gulf Stream. Superimposed on the moored buoy data (circles) are the GPS dropsonde and AXBT data from Hurricane Erika, 1997 (triangles).

Further confirming this relationship are observations from nearly 12 drifting buoys air-deployed ahead of Hurricanes Luis and Marilyn in 1995 and Fran in 1996. Fig 8 shows the relationship between 1-m level measurements of air-sea temperature difference as a function of estimated 10-m wind (from 1-m anemometer measurements). One sees the same increase of air-sea temperature difference with wind speed as in Fig 1, except commencing at a higher wind, a result which may be due to the assumptions inherent in the Liu boundary layer model used for extrapolation. Interpretation of these observations is now much more promising with the successful deployment of the new GPS dropsonde with reliable wind, temperature, humidity and pressure measurements every one-half second to within less than 10 m of the surface. Innovative, successful

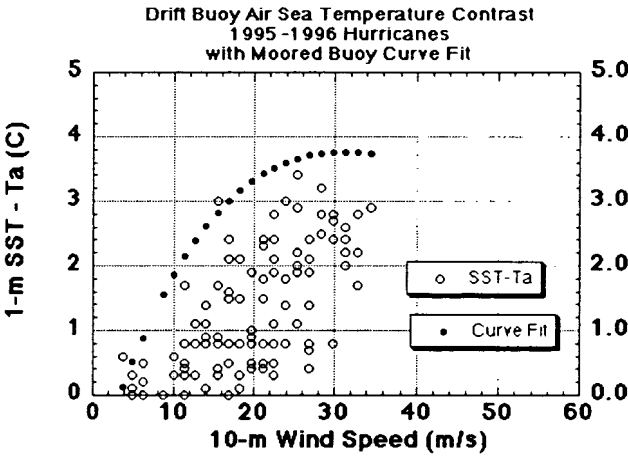


Fig 8. Scatter plot of observations at the 1-m level from drifting buoys in Hurricanes Luis and Marilyn in 1995 and Fran in 1996. Regression curve from Fig 7 is superimposed.

deployments of these sondes were made for the first time NOAA WP-3D and G-IV aircraft in the inner core of EPAC Hurricane Guillermo (1997) by James Franklin and Michael Black or HRD. Additional deployments were made on 3 days in Hurricane Erika.

Preliminary analysis of a few of the eyewall soundings have revealed several new and unusual boundary layer structures. Shown schematically in Fig. 9a, three eyewall soundings indicate low-level wind maxima below 100 m. Fig 9b illustrates the consistency among the three soundings of these features in vertical profiles of dry static energy, specific humidity and wind speed. They show elevated specific humidity in a thin layer below the wind maxima. Nearly all high wind soundings show this feature. Most eyewall soundings also showed a deeper layer of constant theta, or dry static energy. Many soundings show a second wind maximum above this layer near 1200 m. These wind observations are consistent with Australian tower observations in the inner, high-wind core of tropical cyclones first reported by Wilson (1979) and recently discussed by Kepert and Holland (1997). These data showed a low level wind maximum consistently at the 60-m level, as well as a wind maximum near the top of the 400-m tower.

The observation of a thin layer of elevated specific humidity in the high wind region beneath the eyewall is very suggestive of a spray layer which may enhance evaporation in the >90% relative humidity air. The existence of a wind maximum above this layer indicates that upward vapor fluxes in the boundary layer may be controlled more by shear-induced turbulence at the top of the high specific humidity layer than by direct flux from the sea. Sea spray processes such as discussed by Fairall, et al (1994) may become important. Additional analysis of this revolutionary new data source should lead to profound new insights into the workings of the hurricane eyewall boundary layer.

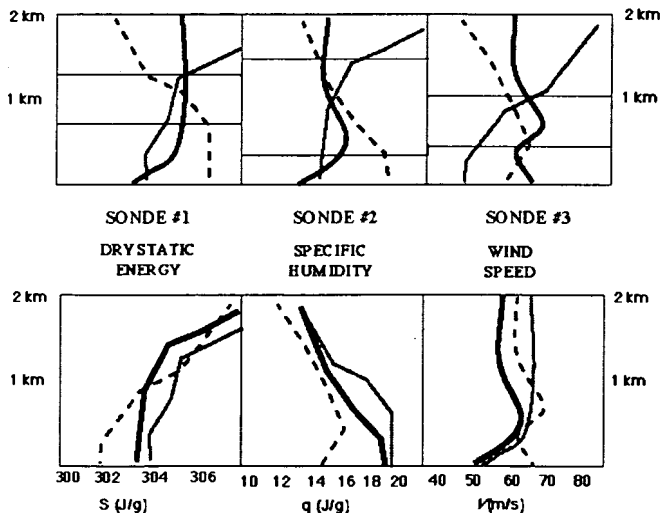


Fig. 9. GPS dropsonde profiles of dry static energy, mixing ratio and wind speed for the north eyewall of Hurricane Guillermo arranged by sounding (a) and by parameter (b).

7. REFERENCES

- Black, P. G., G. J. Holland and V. Pudov, 1993: Observations of sea-air temperature difference in tropical cyclones as a function of wind speed: Importance of spray evaporation. Abstract only. *20th Conference On Hurricanes and Tropical Meteorology*, San Antonio, TX, 10-14 May, 1993.
- Black, P. G., 1983: Ocean temperature changes induced by tropical cyclones. Ph.D. Dissertation, The Pennsylvania State University, State College, PA, 278p.
- Bosart, L. F., W. E. Bracken, J. Molinari, P.G. Black, and C. S. Velden: 1998: Environmental influences on the rapid intensification stage of hurricane Opal (1995) over the Gulf of Mexico. *Proc. Tropical Cyclone Symposium*, AMS 78th Annual Mtg., Phoenix, AZ, 11-16 Jan, 1998.
- Cione, J. J. and P. G. Black, 1998: Surface temperature observations within the tropical cyclone inner core. *Proc. Tropical Cyclone Symposium*, AMS 78th Annual Mtg., Phoenix, AZ, 11-16 Jan, 1998.
- Fairall, C. W., J. D. Kepert and G. J. Holland, 1994: The effect of sea spray on surface energy transports over the ocean. *The Global Atmosphere and Ocean System*, **2**, 121-142.
- Gray, W. M., 1995: Limiting influences on the maximum intensity of tropical cyclones. *Proc. 21st Conference on Hurricanes and Tropical Meteorology*, Miami, FL, 24-28 April, 368-370.
- Holland, G. J., 1997: Maximum potential intensity of tropical cyclones. *J. Atmos. Sci.*, in press.
- Kepert, J. D. and G. J. Holland, 1997: The Northwest Cape tropical cyclone boundary layer monitoring station. *Proc. 22nd Conference on Hurricanes and Tropical Meteorology*, Ft. Collins, CO, 19-23 May, 82-83.
- Korolev, V. S., S. A. Petrechenko and V. D. Pudov, 1990: Heat and moisture exchange between the ocean and atmosphere in Tropical Cyclones Tess and Skip. *Soviet Meteorol. and Hydrol.*, **3**, 92-94 (English edition).
- Jarrell, J. D., P. J. Hebert and M. Mayfield, 1992: Hurricane experience levels of coastal county populations from Texas to Maine. NOAA Tech. Memo. NWS NHC-46, 152 pp.
- Neumann, C., H. Nicholson, C. Guard, 1997: National Plan for Tropical Cyclone Research and Reconnaissance (1997-2002), FCM-P25-1997, Office of the Federal Coordinator for Meteorological Services and Supporting Research.
- Powell, M. D., 1980: Evaluations of diagnostic marine boundary layer models applied to hurricanes. *Mon. Wea. Rev.*, **108**, 757-766.
- Powell, M. D., S. H. Houston and T. A. Reinhold, 1996: Hurricane Andrew's landfall in South Florida. Part I: Standardizing measurements for documentation of surface windfields. *Wea. and Forecasting*, **11**, 304-327.
- Powell, M. D. and S. H. Houston, 1996: Hurricane Andrew's landfall in South Florida. Part II: Surface windfields and potential real-time applications. *Wea. and Forecasting*, **11**, 329-349.
- Pudov, V. D. and G. J. Holland, 1997: Typhoons and the ocean: Results of experimental investigations. Bureau of Meteorology Research Center, BMRC Research Report No. 45, 320pp.
- Pudov, V. D. and S. A. Petrechenko, 1988: Temperature of the South China Sea, *Meteorologija Gigrologija*, **12**.
- Shay, L. K., G. J. Goni, F. D. Marks, J. J. Cione and P. G. Black, 1998: Role of warm ocean features on intensity change: Hurricane Opal. *Proc. Tropical Cyclone Symposium*, AMS 78th Annual Mtg., Phoenix, AZ, 11-16 Jan, 1998.
- Shay, L. K., A. J. Mariano, S. D. Jacob, and E. Ryan, 1997: Mean and near-inertial ocean current response to hurricane Gilbert. *J. Phys. Oceanogr.* (in press).
- Shay, L. K., P. G. Black, A. J. Mariano, J. D. Hawkins and R. L. Elsberry, 1992: Upper ocean response to hurricane Gilbert. *J. Geophys. Res.*, **97**(12), 20,227-20,248.
- Sheets, R. H., 1990: The National Hurricane Center, past, present and future. *Wea. and Forecasting*, **5**, 185-232.
- Willoughby, H. E. and P. G. Black, 1996: Hurricane Andrew in Florida: Dynamics of a disaster. *Bull. Amer. Meteorol. Soc.*, **77**, 543-549.
- Willoughby, H. E., J. A. Clos and M. G. Soreibah, 1982: Concentric eye walls, secondary wind maxima and evolution of the hurricane vortex. *J. Atmos. Sci.*, **39**, 189-200.
- Wilson, K. J., 1979: Characteristics of the subcloud layer wind structure in tropical cyclones. International Conf. on Tropical Cyclones, Perth, Australia.
- Xie, L., L.J. Pietrafesa, E. Bohm, C. Zhang, X. Li, 1998: Evidence and mechanism of hurricane fran-induced ocean cooling in the charleston trough. *Geophys. Res. Lett.*, submitted.

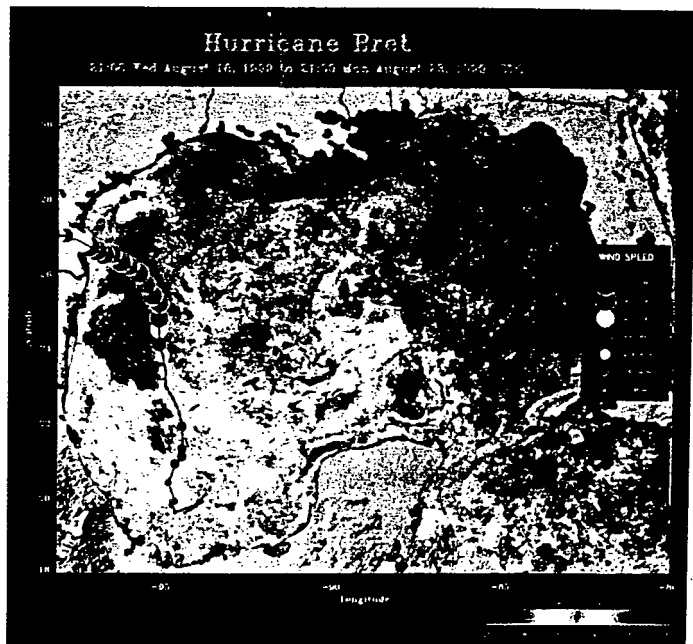
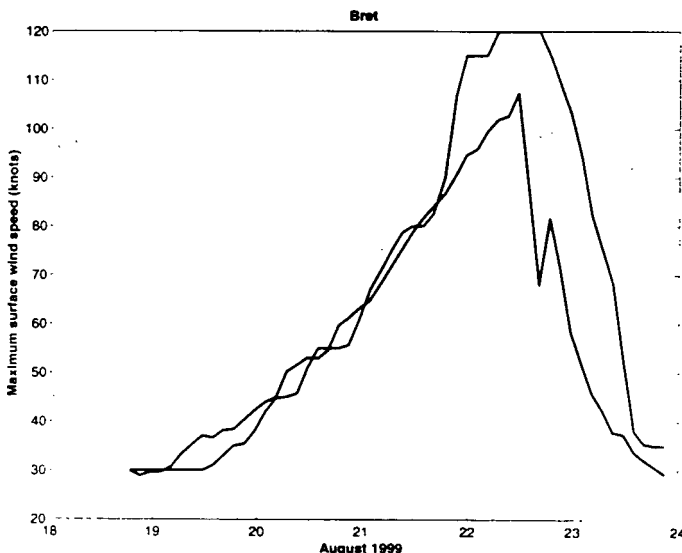
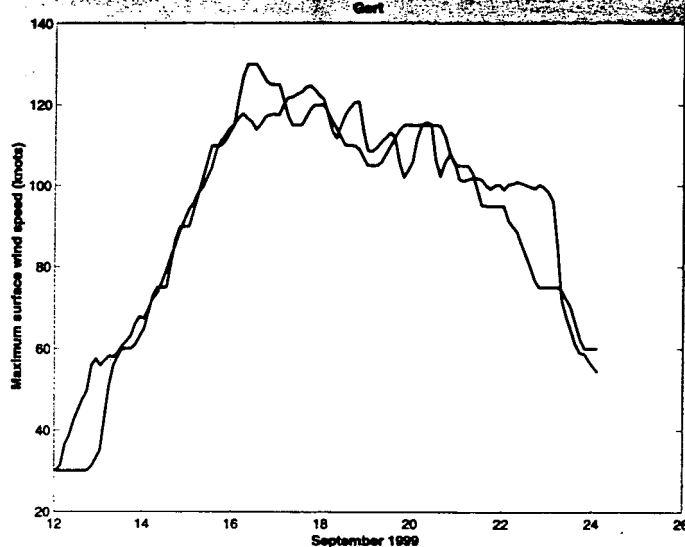
Reference No. 3:

Cione, J.J., P. Molina, J. Kaplan, and P.G. Black, SST Time Series Directly Under Tropical Cyclones: Observations And Implications *Proceedings, 24th Conference on Hurricanes and Tropical Meteorology*, pp. 1-2, Boston, MA: American Meteorological Society (2000).

24th Conference on Hurricanes and Tropical Meteorology

29 May – 2 June 2000

Fort Lauderdale, F



AMERICAN
METEOROLOGICAL
SOCIETY

1A.1 SST TIME SERIES DIRECTLY UNDER TROPICAL CYCLONES: OBSERVATIONS AND IMPLICATIONS

Joseph J. Cione*, Paulo Molina, John Kaplan and Peter G. Black

NOAA/AOML/Hurricane Research Division
Miami, FL

1. INTRODUCTION

It is widely recognized that hurricanes draw their energy from the sea. It has also been observed that hurricanes can significantly modify the ocean thermal structure over which they travel (Black 1983). In fact, upper ocean "cold wakes" are often observed along the track of Tropical Cyclones (TC) and are typically 4-5°C cooler than surrounding "ambient" sea surface temperatures (SST). However, what is not nearly as well documented is exactly how much of this ~4-5°C cooling occurs *directly under the storm within the hurricane inner core environment*. This is an important question which to date, has been difficult to accurately assess. Much of the oceanographic data obtained in earlier TC studies has been ~ instantaneous in nature (i.e. AXBT, AXCP and AXCTD derived data). Another issue complicating matters is that "continuous data platforms" (such as drifting or moored buoys) often fail to collect data when exposed to the extremely harsh oceanic environment within the hurricane inner core. Nevertheless, over the past 25 years there have been several instances where buoys have survived these extreme conditions and successfully recorded near surface oceanographic and meteorological data (Cione et al. 2000). It is a main goal of this study to quantitatively document SST changes *observed under the storm* using data from these infrequently obtained TC-buoy time series. Preliminary findings as well as initial implications with regard to TC intensity change will be presented.

2. METHODOLOGY AND DATA

The primary data source for this study is the TC-Buoy Database (TCBD) recently developed and utilized by Cione et al. (2000). The version of the TCBD used in this research incorporates near-surface meteorological and oceanographic observations from 135 time series obtained from the National Data Buoy Center's (NDBC) moored and drifting buoys and coastal marine automated network (CMAN) platforms. In all, the TCBD includes observations from 37 hurricanes over a 23-year period between 1975-1998. In addition to the surface meteorological and oceanographic data, the TCBD also incorporates information on hurricane center position, minimum sea level pressure and maximum surface wind speed (Neumann et al. 1993).

For this study, two measurement techniques were used to estimate SST change under the storm. The first method developed was the 'complete time series method' (CTSM). Using this technique, SST change was obtained by measuring SST at specific radial distances (RD) from the storm center. First as the storm approached and then again

as the TC departed the buoy. Another stipulation was that at its closest passage the storm had to come inside 0.5 RD of the observing platform. Also, only buoys and TC center fixes south of 35°N were included. A statistical summary of the 1 RD CTSM is given in Table 1. After sorting by SST change, upper and lower 50% samples were created. These results are also presented in Table 1.

3. SUMMARY OF PRELIMINARY RESULTS

The most noticeable attribute listed in Table 1 is the difference in initial TC intensity (TCI(i)) between the upper and lower 50% groupings. True differences between these two means were found to be statistically significant at the 95% level.

Due to the relatively low number of time series that resulted when using the CTSM, a second method was designed in order to significantly increase the sample size. This technique, called the 'six hour method' (6hM) measured SST change over a 6 h period. Here, TC-to-buoy distance had to be inside 2.5 RD, initial SST was at least 27°C and similar to the CTSM, only buoys and TC center fixes south of 35°N were included. A statistical summary of results using the 6hM are presented in Table 2.

TABLE 1. Statistical Summary using the Complete Time Series Method for 1 RD Events

	DEL SST (°C)	Buoy Lat (deg)	Max buoyV (ms ⁻¹)	TCI p(I)	SST (i) (°C)	TC spd (ms ⁻¹)	DEL TCI (mb)
All 1 RD DEL SST							
Min	-3.9	14.2	13.7	922	25.1	2.4	-25.0
Max	0.0	32.7	47.3	1002	29.7	12.9	33.0
Mean	-0.66	27.43	27.0	968.4	27.9	7.0	-2.6
St dev	0.78	4.00	7.00	20.5	1.40	2.21	10.4
Count	29	28	29	29	29	26	29
TOP 50% DEL SST							
Min	-0.4	14.2	13.7	922.0	25.1	4.7	-25.0
Max	0.0	32.51	47.3	988.0	29.3	9.4	7.0
Mean	-0.24	26.08	26.4	960.2	27.8	7.0	-3.2
St dev	0.15	4.85	8.16	21.64	1.41	1.53	8.51
Count	14	14	14	14	14	13	14
BOT 50% DEL SST							
Min	-3.9	24.61	17.6	946.0	25.2	2.4	-18.0
Max	-0.4	32.72	37.3	1002	29.7	12.9	33.0
Mean	-1.10	28.78	27.6	976.0	27.9	7.0	-2.0
St dev	0.91	2.41	5.97	16.66	1.44	2.80	12.26
Count	15	14	15	15	15	13	15

Left aligned bold values denote statistical significance at the 95% level

*Corresponding author's address: Joseph J. Cione, NOAA AOML-HRD, 4301 Rickenbacker Causeway, Miami, FL 33196; e-mail address: cione@aoml.noaa.gov

TABLE 2. Statistical Summary using the 'Six Hour Method' for observations inside 2.5 RD

	DEL SST (°C)	Buoy Lat (deg)	Avg. buoyV (ms ⁻¹)	TCI p(i) (mb)	SST (i) (°C)	TC spd (ms ⁻¹)	DEL TCI (mb)
ALL DEL SST 6h							
Min.	-2.3	14.18	3.5	922	27	1.5	-34
Max.	0	34.68	50.4	1002	30.6	18.3	32
Mean	-0.28	27.55	17.8	970.6	28.4	5.8	-2.3
St dev	0.34	3.78	4.91	18.4	0.77	2.34	5.82
Count	932	932	920	903	916	694	903
DEL SST = 0 °C							
Min.	0	14.18	7.4	922	27.1	1.8	-23
Max.	0	34.68	31.4	996	29.9	16	14
Mean	0	27.16	17.1	962.8	28.3	6.7	-2.3
St dev	0	4.49	4.28	18.9	0.71	2.73	5.4
Count	242	242	242	233	226	161	233
BOT 25% DEL SST < 0 °C							
Min.	-2.3	24.46	9.8	933	27	1.5	-16
Max.	-0.4	34.68	50.4	1002	30.6	13.2	32
Mean	-0.69	28.82	18.6	976.4	28.4	5.5	-1.3
St dev	0.36	2.64	5.41	15.4	0.81	2.07	6.4
Count	280	280	269	274	280	205	274

Left aligned bold (bold and italic) values denote statistical significance at the 95% (99%) level

Similar to the results shown in Table 1, statistically significant differences in SST change ('DEL SST') exist between the 'DEL SST = 0°C' and 'BOT 25% DEL SST < 0°C' subgroups (herein referred to as 'DSST₀' and 'BigDSST25%', respectively). In addition (and unlike research found in Table 1), comparisons of other mean parameters between the two subgroups were also found to be statistically significant. Statistically significant values at the 95% level are left justified and bold while 99% values are left justified, bold and italicized.

Results from both Table 1 and 2 clearly show that large SST cooling events are associated with weaker initial TCs. On average, these weaker storms were at higher latitudes and were moving slower (6hM analyses only). Both of these findings would suggest a higher potential for SST cooling for the BigDSST group since the depth of the oceanic mixed layer tends to decrease with increasing latitude (Mayer et al. 1998) while slower TC motion tends to increase ocean mixing which in turn reduces SST (Black 1983; Shay et al. 1992). BigDSST's stronger average surface winds would also tend to increase ocean mixing and reduce SSTs.

It is also worth noting that the average *initial SST* is nearly identical for all groups listed in Tables 1 and 2. This is an important point and further illustrates how pre-existing *initial SST* cannot be used as a predictive measure for subsequent TC intensity change (Shay et al. 2000). Nevertheless results from Table 2 may suggest a possible linkage between SST change and TC intensity

change. In fact, Figure 1 expands upon the statistically significant relationship illustrated in Table 2 between BigDSST 'DEL TCI' and DSST₀ 'DEL TCI' and also includes DEL SST and DEL TCI average values from the bottom 10% (BigDSST10%) and 5% (BigDSST5%) of the DEL SST < 0°C population sample.

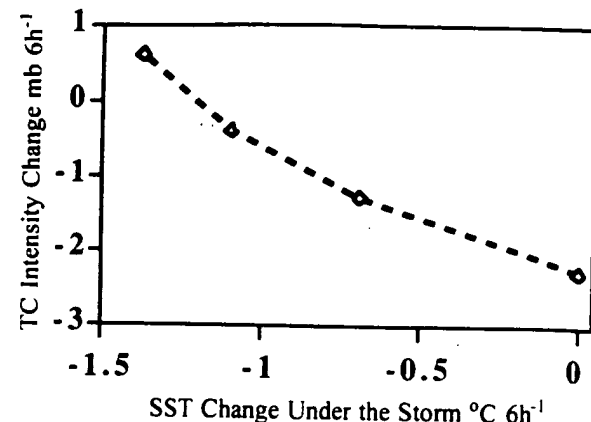


Figure 1: SST change under the storm (°C 6h⁻¹) vs. TC intensity change (mb 6h⁻¹). This graph includes average values of both quantities using the 'six hour method' for the following subgroups: DSST₀, BigDSST25%, BigDSST10% and BigDSST5%.

While the magnitude of the signal illustrated in Figure 1 is relatively weak (i.e. max 2-3mb 6h⁻¹), its coherent structure is both significant and somewhat surprising given the relative short averaging time (6h) and fact that TC intensity change often incorporates several interacting dynamic processes (only one of which is TC-ocean interaction).

4. REFERENCES

- Black, P. G., Ocean temperature changes induced by tropical cyclones. Ph.D. dissertation. 278 pp.. Pa. State Univ., State College, 1983.
- Cione, J.J., P. J. Black and S. Houston 2000: Surface observations in the hurricane environment. *Mon. Wea. Rev.* (in press).
- Mayer, D. A., R. L. Molinari, and J. F. Festa 1998: The mean and annual cycle of upper layer temperature fields in relation to Sverdrup dynamics within gyres of the Atlantic Ocean. *J. Geophys. Res. Phys.* **103**, 18.545-18.566
- Neumann, C.J., B.R. Jarvinen, C. J. McAdie, and J.D. Elms, 1993: Tropical cyclones of the north Atlantic Ocean, 1871-1992. *Hist. Clim.Series* 6-2. Nat. Climat. Data Center, Asheville, NC, 193 pp.
- Shay, L. K., G. J. Goni, and P.G. Black, 2000: Effect of a warm core ocean ring on hurricane Opal. *Mon. Wea. Rev.* (in press).
- Shay, L. K., P.G. Black, A. J. Mariano, J. D. Hawkins and R. L. Ellsberry 1992: Upper ocean response to hurricane Gilbert. *J. Geophys. Res. Phys.* **97**, 20.2227-20.248.

Reference No. 4:

Emanuel, K., Thermodynamic Control of Hurricane Intensity, *Nature*, Vol. 401, pp. 665-669 (1999).

Thermodynamic control of hurricane intensity

Kerry A. Emanuel

Program in Atmospheres, Oceans, and Climate, Massachusetts Institute of Technology, Cambridge, Massachusetts 02139, USA

To establish useful warning systems for hurricanes, it is necessary to accurately predict both hurricane intensity and track. But although the forecasting of hurricane tracks has improved over the past 30 years, the factors that control the intensity of hurricanes are still poorly understood, leading to almost no reliability in forecasts of hurricane intensity evolution. Efforts to improve intensity forecasts have focused almost exclusively on characterizing the dynamical interactions between hurricanes and their atmospheric environment. Here I use a simple numerical model to demonstrate that, in most cases, the evolution of hurricane intensity depends mainly on three factors: the storm's initial intensity, the thermodynamic state of the atmosphere through which it moves, and the heat exchange with the upper layer of the ocean under the core of the hurricane. Such a limited number of controlling factors offers hope that, given an accurate forecast of a hurricane's track, its intensity can be reliably forecast using very simple models.

Forecasts of the tracks of hurricanes have improved steadily over the past three decades¹, owing to a combination of better observations and much improved numerical models. These improvements, coupled with advances in warning systems and preparedness for emergencies, have brought about a significant decline in loss of life in the USA in spite of a near doubling of the coastal population during this period. At the same time, the economic vulnerability to hurricanes has increased dramatically. It has been estimated² that a repeat of the Miami hurricane of 1926 would incur \$75 billion in insured loss, compromising the entire US insurance industry. Among the many costs associated with hurricanes is the expense of evacuation. In practice, many more people are evacuated than was necessary in hindsight, owing to uncertainties in the forecast of both the track and intensity of the storm. Evacuation in the face of a marginal hurricane is usually unnecessary, but is often carried out because hurricanes can intensify rapidly and unexpectedly.

In contrast to the improvement in track forecasts, there has been comparatively little advance in predictions of intensity¹ (as measured, for example, by maximum surface wind speed), in spite of the application of sophisticated numerical models. The best intensity forecasts today are statistically based³. Most of the research literature on hurricane intensity focuses on the pre-storm sea surface temperature and certain properties of the atmospheric environment, such as the vertical shear of the horizontal wind and dynamical features such as disturbances in the upper troposphere⁴. This remains so, even though it is well known that hurricanes alter the surface temperature of the ocean over which they pass⁵ and that a mere 2.5 K decrease in ocean surface temperature near the core of the storm would suffice to shut down energy production entirely⁶. Simulations with coupled atmosphere–ocean models^{6–8} confirm that interaction with the ocean is a strong negative feedback on storm intensity. During the Atlantic hurricane season of 1998, guidance based on coupled-model simulations was provided to forecasters for the first time.

Although there is much hope that three-dimensional coupled models will lead to better understanding of the factors that control hurricane intensity and to increased reliability ('skill') of hurricane intensity forecasts, the present generation of models may not have enough horizontal resolution to capture the full intensity of extreme storms. (Fortunately, it is probably not necessary to capture full storm intensity in order to achieve a good track forecast.)

Here I show that an accurate account of the evolution of storm intensity can be achieved using a very simple coupled ocean–atmosphere model in which the atmospheric component is cast in

a transformed radial coordinate that greatly increases horizontal resolution in the critical region around the eyewall, the ring of intense convection that surrounds the eye of the storm. This is so even though the atmospheric component is axisymmetric and therefore excludes interactions with vertical wind shear and dynamical features of the atmospheric environment. This demonstrates that, once storm genesis has occurred, much of the evolution of storm intensity is controlled by its initial intensity together with the thermodynamic properties of the atmosphere and upper ocean along the storm track.

The model

The atmospheric model assumes that the storm is axisymmetric, and that the airflow is never very far from a state in which the horizontal and vertical pressure gradient accelerations are balanced by centrifugal and gravitational accelerations, respectively. It also assumes that the vortex is always close to a state of neutral stability to a combination of gravitational and centrifugal convection ("slantwise convection"⁹). These constraints place very strong restrictions on the structure of the vortex so that, with the exception of the water-vapour distribution, the vertical structure is determined by a very limited set of variables. Moist convection is represented by one-dimensional plumes whose mass flux is determined in such a way as to ensure approximate entropy equilibrium of the boundary layer. The model variables are cast in "potential radius" coordinates¹⁰. Potential radius (R) is proportional to the square root of the absolute angular momentum per unit mass about the storm centre and is defined by $fR^2 = 2rV + f^2$, where V is the velocity of air flowing around the storm, r is the physical radius and f is the Coriolis parameter, which is twice the local vertical component of the Earth's angular velocity.

In the runs presented here, there are 50 nodes that span 1,000 km, giving an average resolution of 20 km; however, the resolution is substantially finer than this in regions of high vorticity, such as the eyewall. A complete description of the model is given elsewhere¹¹. When run with a fixed sea surface temperature and a fixed atmospheric environmental temperature profile, and provided that the vortex specified at the start of the model integration is strong enough, the model vortex amplifies over a period of 4–5 days right up to its potential intensity (see upper curve in Fig. 1a). The potential intensity is the maximum steady intensity a storm can achieve based on its energy cycle, in which the heat input by evaporation from the ocean, multiplied by a thermodynamic efficiency, is balanced by mechanical dissipation in the storm's

= 4.5°F

atmospheric boundary layer¹². It is given by

$$V^2 = \frac{C_k T_s - T_o}{C_D T_o} (k_s - k_a) \quad (1)$$

where V is the maximum wind speed, C_k and C_D are dimensionless exchange coefficients for enthalpy and momentum, T_s and T_o are the absolute temperatures of the sea surface and storm top, and k_s and k_a are the specific enthalpies of the air at saturation at the ocean surface and ambient boundary layer air, respectively. (That the outflow rather than inflow temperature appears in the denominator of equation (1) is due to the fact that the dissipative heating in the storm's boundary layer recycles some of what would otherwise be waste heat back into the thermodynamic cycle of the storm¹³.

Whereas model storms usually spin up to their potential intensity and remain at that intensity indefinitely, real hurricanes seldom behave that way; in fact most hurricanes experience a sharp decline shortly after achieving their peak intensity¹⁴. Moreover, very few real storms ever achieve the potential intensity given by equation (1). From records of previous storms together with the climatology of potential intensity, there is a nearly uniform probability that a given

hurricane will achieve any intensity between marginal hurricane force and the potential intensity¹⁴.

The axisymmetric hurricane model is coupled to a one-dimensional ocean model in a unique way. First, it is assumed that the hurricane responds principally to sea surface temperature changes under its eyewall, and that these can be closely approximated by sea surface temperature changes under that part of the eyewall that lies along the storm track. Second, the evolution of sea surface temperature along the storm track up until the time that the centre of the storm arrives can be approximated as arising entirely from one-dimensional stirring of each vertical column, with no influence from its neighbours. (The horizontal exchange of enthalpy between oceanic columns is ignored.) Finally, the mixing is approximated by assuming that a bulk Richardson number, relating the velocity of the ocean's mixed layer to the jump in temperature across the base of that layer, remains constant¹⁵ as the ocean mixed layer is accelerated by the wind stress imposed from the passing storm. Thus the ocean model consists merely of a set of one-dimensional ocean columns along the storm track, whose temperature is changed only through vertical mixing in each column. The temperature stratification

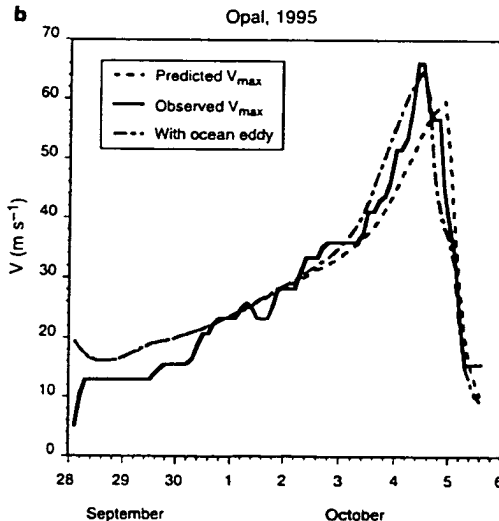
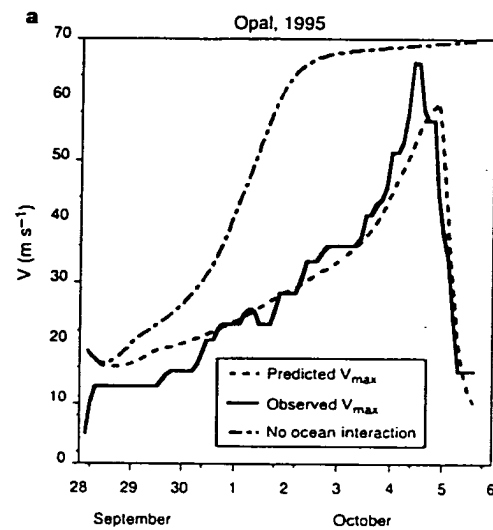


Figure 1 Evolution of the maximum wind speed in Hurricane Opal. In a, the solid line shows the observed evolution, the dashed line shows the modelled evolution, and the dash-dot line shows evolution modelled without ocean interaction. In b, the dash-dot line shows evolution modelled in the presence of a warm ocean eddy.

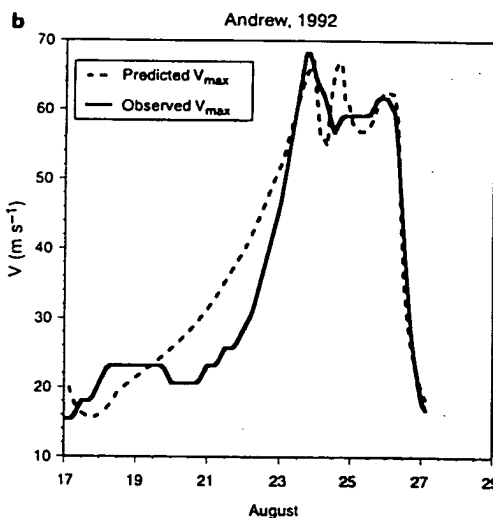
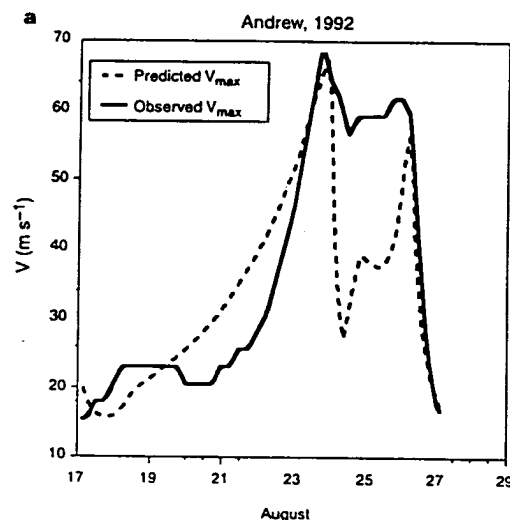


Figure 2 Evolution of the maximum wind speed in Hurricane Andrew. Solid lines are observations and dashed lines are modelled values. The nominal model run is shown in a, while the run in b takes into account the swamp in southern Florida and the shallow continental shelf to its west (see text for details).

below the mixed layer is set to a constant in the runs described here. This very simple formulation has been shown to lead to a storm intensity evolution that is virtually indistinguishable from that of the same hurricane model coupled to a three-dimensional ocean model, in the case of a steadily moving storm¹⁶.

For each event, the model is initialized using a synthetic warm-core vortex. In each of the cases discussed below, the geometry of the vortex is identical, though in principle it can be varied according to the size of the real system. The maximum wind speed of this initial vortex is matched to the observed wind speed at the beginning of the initial period of intensification of the observed system. Also, the initial degree of saturation of the inner storm core is specified so as to achieve the observed, initial rate of intensification. These are crucial steps, as the subsequent evolution is quite sensitive to the initial state. Apart from this initial matching of the model and observed maximum wind speeds, no adjustment of the model vortex towards observations is made.

Two properties of the storm's environment along its observed track are specified from monthly mean climatology: the potential maximum wind speed¹⁷ and the ocean mixed-layer depth¹⁸. The former is interpolated from the 2.5° grid on which it was supplied to the observed storm position; the latter was similarly interpolated from a 1° grid to the observed storm position. Both data sets were

also linearly interpolated to the actual date, assigning the monthly mean climatology to the 15th day of each month. These monthly climatologies were formed using many years of data; no year-to-year variations are accounted for. A third data set, on a 1° grid, was also used to specify ocean depths along the observed storm track. This was used to detect landfall, and also to reveal those situations when the ocean mixed layer extends right to the ocean floor, so that surface cooling by mixing cannot occur. The landfall algorithm is one of maximum simplicity: when the centre of the storm passes over land, the coefficient of surface enthalpy flux is set to zero everywhere. Although this is unrealistic, in practice the strongest effects are under the eyewall, whose passage over land occurs nearly at the same time that the storm centre makes landfall. (The small differences in timing are comparable to the six-hour temporal resolution of the observational data.)

In each of the cases presented below, the evolution of maximum surface wind speed in the model is compared to the observed evolution; no attempt has been made to compare the evolutions of model and observed storm structure, as the latter is not available in any convenient form. It should be borne in mind that not all of the reported wind speeds are directly measured by aircraft or radar; some are partially subjective estimates based on satellite imagery. (Here again, the readily available data archive does not document

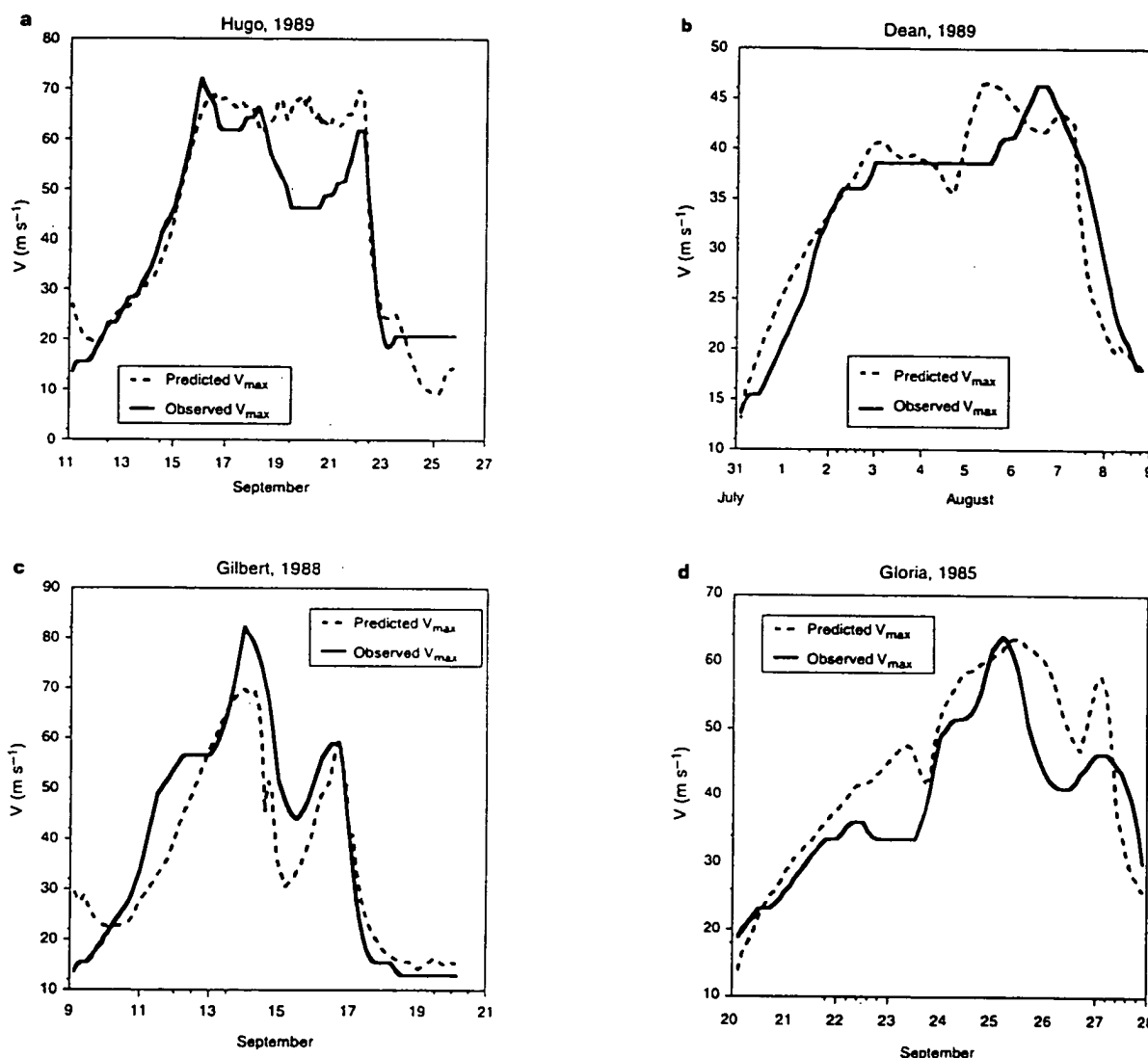


Figure 3 Evolution of maximum wind speed in several hurricanes. **a**, Hurricane Hugo; **b**, Hurricane Dean; **c**, Hurricane Gilbert; and **d**, Hurricane Gloria. In all cases the predicted

and the observed maximum wind speeds are shown by dashed and solid lines, respectively.

the source of the data, but it is safe to assume that most reported wind speeds in storms within one day of landfall in the USA are based on reliable *in situ* or radar measurements within six hours of the reporting time.)

Model skill

Some well simulated examples. Figure 1 shows the observed and modelled evolution of Hurricane Opal, which moved through the Gulf of Mexico in October, 1995, making landfall in northwestern Florida. Also shown in Fig. 1a (but not in subsequent figures) is the evolution that would have occurred had the ocean temperature remained fixed in time, demonstrating the crucial role of ocean interaction. Previous studies of this event have emphasized the role of an approaching upper-tropospheric disturbance⁴ or the observed presence of a warm ocean eddy at about the time of maximum intensification, but Fig. 1a shows that most of the evolution can be accounted for without these effects (I. Ginis, personal communication). The main influence of the approaching upper-tropospheric disturbance was to accelerate the forward motion of the storm, thereby decreasing the ocean cooling. Insertion into the model of a warm ocean eddy of about the dimensions and magnitude of that observed did result in a small but noticeable increase in the peak intensity of the storm, as shown in Fig. 1b.

Hurricane Andrew developed east of the Bahamas in August, 1992, and then moved westward across the southern tip of Florida, into the Gulf of Mexico, and then northwestward, making landfall again in Louisiana. It was the most expensive natural disaster in US history, incurring more than \$28 billion in damage. The evolution of Hurricane Andrew's intensity is shown in Fig. 2a. Here the modelled evolution departs noticeably from the observed in several respects. In its early stages, the model storm intensifies while the observed storm in fact weakens. Operational forecasters at the time attributed this weakening to the presence of substantial vertical wind shear, an effect not accounted for in this model. More spectacularly, the model intensity declines far more rapidly than observed after making landfall in southern Florida. Two important model deficiencies may come into play here: first, the southern tip of Florida is not dry land but rather a swamp, so that the assumption of vanishing surface heat flux may be extreme. Second, the resolution of the ocean depth data set was not high enough to account accurately for the presence of a shallow shelf extending westward from the southern tip of Florida. In reality, the ocean mixed layer over which Hurricane Andrew moved probably extended right to

the sea floor for the first ten hours or so after the storm left Florida. In Fig. 2b, the model has been modified to account for the actual depth of the sea floor along the storm track, and the surface enthalpy exchange coefficient has been reduced by only one-half while the storm is over southern Florida. This illustrates how very sensitive hurricane intensity is to the nature of the underlying surface.

Hurricane Hugo moved through the northern Caribbean and then up over the Sargasso Sea, making landfall in South Carolina in September, 1989. Figure 3a compares the actual and modelled storm evolution. The simulation is quite good, except when the storm is over the Sargasso Sea, in which case the model overestimates its actual intensity. There is considerable evidence that Hugo was affected by vertical wind shear during this time.

Hurricane Dean moved westward over the tropical North Atlantic to just north of the Virgin Islands, then turned north, moving over open waters until it struck southeastern Newfoundland in early August, 1989. It never exceeded marginal hurricane intensity. Figure 3b compares the predicted and modelled intensities of that storm.

Hurricane Gilbert, in September 1988, was the most intense hurricane ever recorded in the Atlantic region. It moved westward over the Caribbean Sea, striking Jamaica and the Yucatan peninsula before passing into the Gulf of Mexico. Figure 3c shows that whereas

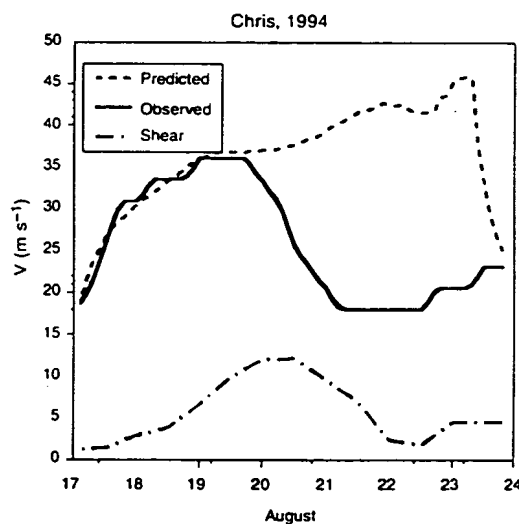


Figure 4 Evolution of the maximum wind speed in Hurricane Chris. The solid line shows observations, and the dashed lines are modelled values; the dash-dot line shows an estimate of the magnitude of the environmental vertical wind shear at the storm centre.

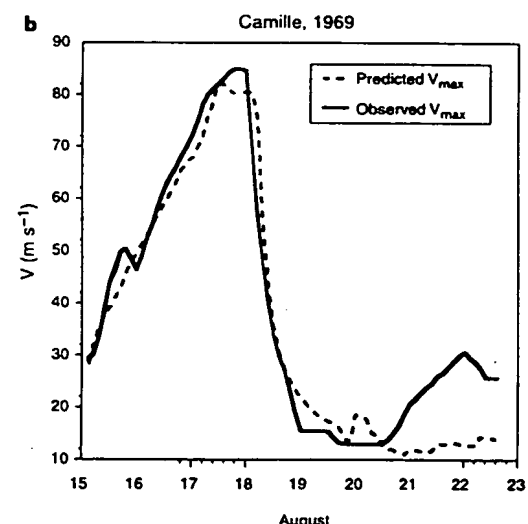
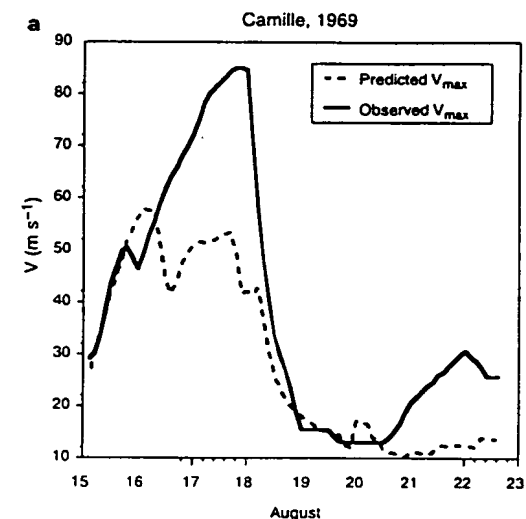


Figure 5 Evolution of the maximum wind speed in Hurricane Camille. Solid lines are observations, and dashed lines are modelled values. The nominal model run is shown in a, while in b the ocean interaction is omitted.

the character of the storm's intensity evolution was well simulated, the peak intensity was substantially underestimated.

Hurricane Gloria formed off Africa, and affected the US east coast in late September, 1985. Figure 3d shows that the evolution of its intensity was well simulated in most respects.

Some notable failures. Especially in their early stages of development, tropical cyclones are susceptible to suppression through the effects of vertical wind shear, or enhancement by dynamical interactions with other weather systems in the high troposphere. These effects have been emphasized in many previous investigations. We have found several examples in which the skill of the present model is significantly compromised by such effects. An example of the first effect is demonstrated by Fig. 4, which shows the model prediction of the wind-speed evolution of marginal hurricane Chris in 1994, together with an estimate of the magnitude of the observed environmental vertical wind shear at the storm centre (J. Kaplan, personal communication). This hurricane appears to have been severely limited by the shear, which reaches its peak intensity just as the hurricane goes into decline. We have also found several cases in which the present model underpredicts the intensity of events that were apparently affected by dynamical interactions with their environment. We emphasize, however, that such effects are significant in only a small fraction of the cases that we have examined.

Figure 5a shows the predicted and observed evolutions of Hurricane Camille of 1969, the only category 5 hurricane to strike the US mainland in the 100-year period of record, making landfall near Biloxi, Mississippi. The intensity of the storm is very badly underpredicted. Figure 5b shows that if the sea surface temperature is held fixed, the simulation is quite good. One of the interesting features of the Gulf of Mexico is the Loop Current, an extension of the Gulf Stream that loops up towards the coast of Alabama and Mississippi but whose exact position is somewhat variable. No manifestation of this current was evident in the climatological ocean data interpolated to the observed positions of Camille. There is some evidence that Camille moved right along the axis of the Loop Current, which has a locally deep, warm mixed layer¹⁹. It has been suggested²⁰ that most of the very severe hurricanes that affect the Gulf coast move along the Loop Current.

Discussion

The simulations presented here suggest that, once tropical cyclones reach tropical-storm strength, their intensity evolution is controlled mostly by their initial intensity together with the thermodynamic profile of the atmosphere and upper ocean through which they move. Factors such as vertical wind shear and dynamical interactions with the environment, emphasized in previous work, appear to be strongly influential mostly during the formative stages, when the storms are comparatively weak. Storm intensity is particularly sensitive to the thermodynamic structure of the upper ocean, and it

is evident that in at least some cases (for example, Hurricane Camille) the climatological specification of the ocean thermal structure is insufficient. Accurate prediction of hurricane intensity in these cases probably requires accurate measurement of the upper-ocean thermal structure ahead of the storm. The simulations presented here offer hope that even with a very simple model, hurricane intensity can be predicted with useful skill as far in advance as an accurate track prediction can be made. Such track predictions require three-dimensional models able to account for the full range of interactions between the storm and its environment. □

Received 6 May; accepted 26 August 1999.

1. DeMaria, M. & Kaplan, J. An operational evaluation of a statistical hurricane intensity prediction scheme (SHIPS). Preprints of the 22nd Conf. on Hurricanes and Tropical Meteorology 280–281 (American Meteorological Soc., Boston, 1997).
2. Landsea, C. W. & Piehlke, R. A. Jr. Normalized hurricane damages in the United States: 1925–95. *Weath. Forecast.* 13, 621–631 (1998).
3. DeMaria, M. & Kaplan, J. A statistical hurricane intensity prediction scheme (SHIPS) for the Atlantic basin. *Weath. Forecast.* 9, 209–220 (1994).
4. Bosart, L. F., Bracken, W. E. & Molinari, J. Environmental influences on the rapid intensification of Hurricane Opal (1995) over the Gulf of Mexico. Preprints of the 23rd Conf. on Hurricanes and Tropical Meteorology 983–984 (American Meteorological Soc., Boston, 1999).
5. Price, J. F. Upper ocean response to a hurricane. *J. Phys. Oceanogr.* 11, 153–175 (1981).
6. Gallacher, P. C., Rotunno, R. & Emanuel, K. A. Tropical cyclogenesis in a coupled ocean-atmosphere model. Preprints of the 18th Conf. on Hurricanes and Tropical Meteorology (American Meteorological Soc., Boston, 1989).
7. Schade, L. R. & Emanuel, K. A. The ocean's effect on the intensity of tropical cyclones: Results from a simple coupled atmosphere-ocean model. *J. Atmos. Sci.* 56, 642–651 (1999).
8. Khain, A. & Ginis, I. The mutual response of a moving tropical cyclone and the ocean. *Beitrage Phys. Atmos.* 64, 125–141 (1991).
9. Emanuel, K. A. The Lagrangian parcel dynamics of moist symmetric instability. *J. Atmos. Sci.* 40, 2368–2376 (1983).
10. Schubert, W. H. & Hack, J. J. Transformed Eliassen-balanced vortex model. *J. Atmos. Sci.* 40, 1571–1583 (1983).
11. Emanuel, K. A. The behavior of a simple hurricane model using a convective scheme based on subcloud-layer entropy equilibrium. *J. Atmos. Sci.* 52, 3959–3968 (1995).
12. Emanuel, K. A. An air-sea interaction theory for tropical cyclones. Part I. *J. Atmos. Sci.* 42, 1062–1071 (1986).
13. Bister, M. & Emanuel, K. A. Dissipative heating and hurricane intensity. *Meteorol. Atmos. Phys.* 65, 233–240 (1998).
14. Emanuel, K. A. A statistical analysis of tropical cyclone intensity. *Mon. Weath. Rev.* 127, (in the press).
15. Price, J. F. Internal wake of a moving storm, Part I: Scales, energy budget, and observations. *J. Phys. Oceanogr.* 13, 949–965 (1983).
16. Schade, L. R. A physical interpretation of SST-feedback. Preprints of the 22nd Conf. on Hurricanes and Tropical Meteorology 439–440 (American Meteorological Soc., Boston, 1997).
17. Bister, M. & Emanuel, K. Hurricane climatological potential intensity maps and tables. (cited 01/05/99) (<http://www-pao.c.mil.edu/~emanuel/pcmr/climo.html>) [22/03/97]
18. Levitus, S. *Climatological Atlas of the World Ocean* (NOAA Prof. Pap. No. 13, US Gov. Printing Office, Washington, DC, 1982).
19. Ly, L. N. & Kantha, L. H. A numerical study of the nonlinear interaction of Hurricane Camille with the Gulf of Mexico loop current. *Oceanol. Acta* 16, 341–348 (1993).
20. Cooper, C. In Proc. Offshore Tech. Conf. 213–222 (Offshore Tech. Conf., Richardson, Texas, 1992).

Acknowledgements

The vertical wind shear data were supplied by Dr. J. Kaplan of the NOAA/ERL Hurricane Research Division. I thank H. Willoughby for comments on the manuscript.

Correspondence and requests for materials should be addressed to K.A.E. (e-mail: emanuel@texmex.mit.edu).

Reference No. 5:

Gentemann, C., D. Smith, and F. Wentz, Microwave SST Correlation With Cyclone Intensity, *Proceedings, 24th Conference on Hurricanes and Tropical Meteorology*, pp. 3-4, Boston, MA: American Meteorological Society (2000).

MICROWAVE SST CORRELATION WITH CYCLONE INTENSITY

Chelle Gentemann*
 Deborah Smith
 Frank Wentz
 Remote Sensing Systems, Santa Rosa, CA

1. INTRODUCTION

The TRMM Microwave Imager (TMI), operational since November 1997, provides cloud-penetrating sea surface temperature (SST) measurements. At its lowest frequency channel (10.7 GHz) the atmosphere is nearly transparent, making it possible to measure SSTs reliably. This channel has little attenuation from non-raining clouds, giving a clear view of the sea surface under all weather conditions except rain. These attributes make TMI SST especially valuable for measuring SST during severe storms when traditional infrared SST retrievals are often thwarted by cloud cover. Using 2 years of data we analyze the effect of SST on storm intensity. Also, post-storm SST anomalies are examined in order to relate intensity to storm-induced upwelling.

2. OCEANIC RESPONSE TO TROPICAL CYCLONES

Infrared (IR) SST observations have been used to study the oceanic response to tropical cyclones. Directly to the right of their track, strong storms leave a cold wake (Monaldo, 1997; Nelson, 1998). The analysis of the cold wakes has been hampered by lack of IR SST retrievals due to cloud cover or contamination by undetected clouds and atmospheric aerosols (Wentz, *submitted*). Retrieval errors in TMI SST are primarily due to both wind speed and direction (Wentz, 1996). The TMI SST algorithm ingests model winds to minimize this effect. The Reynolds SST maps are used by the National Hurricane Center's (NHC) storm intensity forecast models. SSTs exert significant thermodynamic control on the storm intensity (DeMaria, 1994).

Figure 1 compares the TMI SST field with the weekly Reynolds SST of Hurricane Dennis and Cindy on September 3-5, 1999. Figure 1A shows a three day average of TMI SST directly after the passage of two hurricanes (Dennis and Cindy). The cold wake from Dennis can be seen directly alongside the East Coast of North America. Cindy's cold wake is farther offshore, in the top right of Figure 1A. Reynolds SSTs are used in most coupled weather models and in the NHC intensity forecasts. Figure 1B was the weekly map available by September 5, 1999. The upwelling isn't present because 1) the weekly resolution and 2) the satellite IR SST used in Reynolds analysis is unable to measure SST in the vicinity of the storms due to cloud cover.

*Corresponding author address: Chelle L. Gentemann, Remote Sensing Systems, 438 First Street Suite 200, Santa Rosa, CA 95401; e-mail: gentemann@remss.com

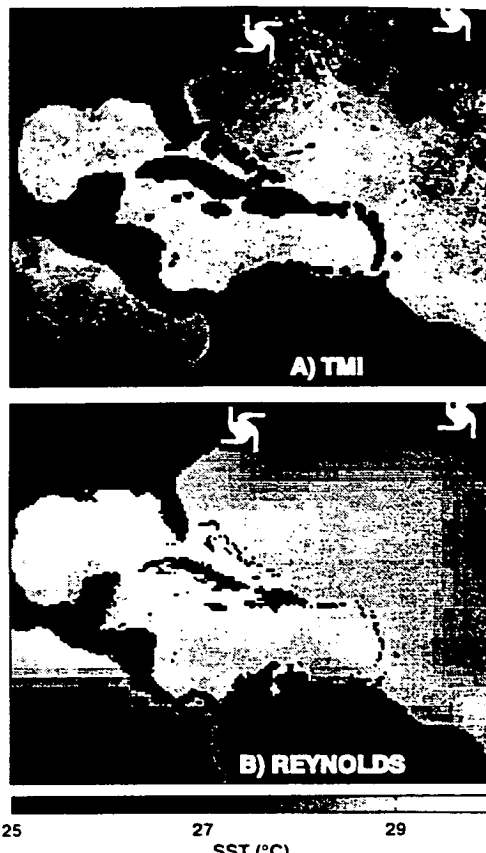


Figure 1. A) TMI SST from September 3-5, 1999. B) Reynolds SST for the week ending August 28, 1999. Positions of Hurricane Dennis and Cindy are indicated by white spiral symbols. Dennis is the leftmost symbol.

3. INTENSITY FORECASTS

Storm track prediction skill has steadily improved along with better numerical models and observations, but intensity prediction skill falls short of expectations (Willoughby, 1999). After initial development, the intensity of severe storms is strongly influenced by the thermodynamic structure of the upper ocean (Emanuel, 1999), and an accurate prediction of the storms future intensity requires measurements of the ocean's thermal structure ahead of the storm. Microwave SST retrievals clearly have the potential to improve skill in these important forecasts (Wentz, *submitted*). Of particular interest, is the spatial/temporal extent to which hurricanes modify SSTs.

Reference No. 6:

Ginnis, I., W. Shen, and M. Bender, Performance Evaluation Of The GFDL Coupled Hurricane Ocean Prediction System In The Atlantic Basin, *Proceedings, 23rd Conference on Hurricanes and Tropical Meteorology*, pp. 607-610, Boston, MA: American Meteorological Society (1999).

PERFORMANCE EVALUATION OF THE GFDL COUPLED HURRICANE OCEAN PREDICTION SYSTEM IN THE ATLANTIC BASIN

Isaac Ginis* and Weixing Shen
 University of Rhode Island Graduate School of Oceanography
 Narragansett, Rhode Island
 Morris A. Bender
 Geophysical Fluid Dynamics Laboratory, NOAA
 Princeton, New Jersey

1. INTRODUCTION

How much we can improve the prediction of tropical cyclone intensity with the use of a coupled tropical cyclone-ocean model? In studies by Bender and Ginis (1998) and Ginis et al. (1997) the GFDL hurricane prediction model was coupled with the Princeton Ocean Model to perform experimental predictions of Hurricane Gilbert (1988) and Opal (1995) in the Gulf of Mexico and Hurricane Felix (1995) and Fran (1996) in the western Atlantic. The results confirmed the conclusions of earlier studies regarding the impact of tropical cyclone-ocean interaction on hurricane intensity. In each of the seven forecasts made, inclusion of the ocean coupling generally led to substantial improvements in the prediction of storm intensity. The obtained results were very encouraging. Subsequently, the GFDL coupled hurricane-ocean prediction system was further tested for more cases in the 1995-97 hurricane seasons. In the beginning of the 1998 hurricane season the coupled system was put in near real time mode when data link with NCEP was established. The framework and performance of the system are briefly described in the present report.

2. THE GFDL COUPLED HURRICANE-OCEAN PREDICTION SYSTEM

The GFDL coupled prediction system is designed for a fully automated performance, in which all steps, the data transfer, model initialization and time integration are conducted without human intervention.

2.1 Data transfer

Input data into the atmospheric component of the prediction system, the GFDL hurricane forecast model (Kurihara et al. 1998), are the National Centers for Environmental Prediction (NCEP) global analysis and the storm message file prepared by the National Hurricane Center (NHC). The oceanic component of the prediction system, the Princeton Ocean Model (Mellor 1996), utilizes the real-time sea surface temperature (SST) analysis produced by NCEP and the monthly averaged profiles of temperature and salinity produced by the NAVOCEANO General Digital Environmental Model

(GDEM). The NCEP SST analysis at 1° resolution consists of all SST observations available to NCEP (e.g. ship and buoy) within 10 hour of observation time, combined with weekly averaged SST retrievals produced by the advanced very high resolution radiometer (AVHRR) carried aboard the NOAA polar orbiting satellites. GDEM is an ocean climatology at 0.5° resolution created from the U.S. Navy observational data base which contains about 5 million observations worldwide dating back to 1920. For each coupled model integration in this study, the input data were transferred via the internet from a Cray C-90 at NCEP to a Cray T-90 at the Naval Oceanographic Office Major Shared Resource Center (MSRC) where all numerical experiments were performed. During the near real time mode forecasts, all necessary data were transferred to MSRC immediately after the integration of the operational GFDL model.

2.2 Model initialization

In the current GFDL initialization procedure used operationally the NCEP global model forecast is used to specify initial environmental fields and the time-dependent lateral boundary conditions. The initial storm structure is estimated from the data in the NHC storm message. The latter provides the target wind field for generation of the tropical cyclone vortex using an axisymmetric version of the prediction model. The symmetric vortex and an asymmetric component determined from the storm structure developed during the previous forecast cycle, are then merged back into the environmental fields determined from the global analysis.

The ocean initialization procedure includes four steps. First, the ocean model is integrated for one month in diagnostic mode (e.g. holding the temperature and salinity constant while allowing the velocity field to evolve in a natural and consistent manner) without surface forcing. This is followed by a three month prognostic run with fixed GDEM climatological SST and wind stress forcing from the Comprehensive Ocean-Atmosphere Data Set (COADS) at the sea surface. These first two phases generate a monthly model climatology on the specified high-resolution grid system for those months for which the hurricane forecasts are made. The third and forth steps of the initialization procedure involve adjusting the upper ocean structure to a more realistic

* Corresponding author address: Dr. Isaac Ginis, Graduate School of Oceanography, University of Rhode Island, Narragansett, RI 02882; e-mail: i.ginis@gso.uri.edu

pre-storm condition at the start of the hurricane forecast. In the beginning of the third step, the NCEP SST data set is assimilated by replacing the GDEM temperatures in the upper ocean mixed layer by the NCEP SSTs and the model is then integrated prognostically for another 10 days for dynamical adjustment. During the final step, the cold wake at the sea surface produced by the hurricane three days prior to the start of the coupled forecast is generated by integrating the ocean model using prescribed hurricane wind stress forcing. A scheme is utilized in which the hurricane's surface wind field is generated using the NHC storm message file.

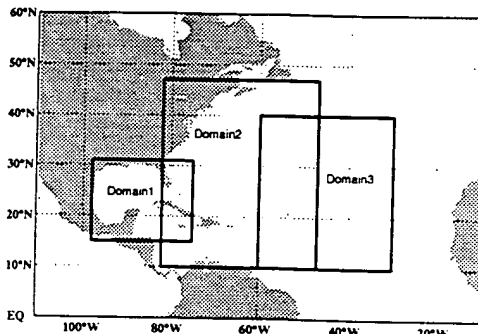


Figure 1. Ocean model domains in the coupled system

2.3 Coupled model design

The coupled hurricane-ocean prediction system consists of the GFDL hurricane model and the Princeton Ocean Model (POM). The GFDL hurricane model is a primitive equation model with 18 sigma-levels in the vertical and a triply-nested movable mesh system in the horizontal (Kurihara et al. 1998). The outermost domain with 1° resolution is stationary during the integrations and ranges from 10°S to 65°N in the meridional direction and is positioned in the zonal direction depending on the storm's initial and 72h official forecast positions. The two inner meshes of 1/3° and 1/6° resolution are movable and follow the storm center.

The POM is a primitive equation ocean model with complete thermohaline dynamics (Blumberg and Mellor 1987). It has a bottom following, sigma coordinate system and a free surface. Three high resolution ocean computational domains of 1/6° resolution were set up for the Gulf of Mexico and the western and central North Atlantic (Fig. 1). At the beginning of each forecast, an appropriate domain is automatically chosen depending on the initial and 72 hour storm positions. The number of vertical levels is set at 21 for the Gulf of Mexico and 23 for the North Atlantic, with higher resolution in the upper mixed layer. All ocean computational domains have 'closed' land-water boundaries and 'open' lateral boundaries where the domains are surrounded by the sea. At the closed boundaries, a no-slip condition is invoked on the velocity field and there are no grid-scale or sub-grid-scale normal fluxes of

any quantity. At the open boundaries, transport and thermal conditions are specified and prescribed according to observations where available.

The method of coupling between the hurricane and the ocean model is similar to the procedure used in Bender et al. (1993). It is performed by passing the wind stress, heat, moisture and radiative fluxes from the atmospheric model to the ocean model, which returns the new SST prediction to the atmospheric model.

Table 1. The GFDL operational and coupled hurricane-ocean model intensity forecast errors in the 1995-97 hurricane seasons. Average absolute errors (in hPa) compared with observed values.

Time	Cases	Errors (hPa)		Impr.(%)
		Oper.	Coupled	
All cases				
12 h	24	8.71	9.01	-3.5
24 h	25	13.61	10.14	25.5
36 h	24	16.84	10.83	35.7
48 h	25	18.12	12.12	33.1
60 h	24	17.01	11.76	30.9
72 h	23	18.02	12.51	30.6
Total	145	15.39	11.06	25.4
Hurricanes ($P_c < 980$ hPa)				
12 h	16	5.63	6.18	-9.8
24 h	16	9.02	5.59	38.0
36 h	18	14.61	7.82	46.4
48 h	19	16.71	9.85	41.0
60 h	20	15.26	10.18	33.3
72 h	20	16.61	11.72	29.4
Total	109	12.97	8.56	29.7
Tropical Storms ($P_c > 980$ hPa)				
12 h	8	14.86	14.68	1.2
24 h	9	21.77	18.22	16.3
36 h	6	23.55	19.84	15.8
48 h	6	22.60	19.29	14.7
60 h	4	25.78	19.65	23.8
72 h	3	27.45	17.79	35.2
Total	36	22.67	18.24	17.8

3. TEST RESULTS

3.1 The 1995-97 hurricane seasons

The automated coupled prediction system was first tested for 32 cases of storms observed during the 1995-1997 seasons. The cases were selected according to the following criteria: the track errors are less than 200 km at 36 hours, and less than 250 km at 72 hours, and the intensity errors are less than 6 hPa at 0 hour. The selected storms were Hurricane Felix - 3 cases, Humberto - 1, Iris - 2, Luis - 7, Marilyn - 2 in 1995; Hurricane Edouard - 2, Fran - 4, Isidore - 3, Lili - 3 in 1996 and Hurricane Erica - 3 in 1997. In most of those cases (about 90 %) the operational GFDL model overpredicted the intensity of the storms measured by central pressure. The coupled system produced very favorable

results for intensity prediction. The mean absolute error of the forecast central pressure was reduced by about 25 %. More detailed error statistics at every 12 hr forecast interval are presented in Table 1. Reduction of the intensity forecast error, compared against the operational GFDL model is significant throughout the entire 72 hour forecast period. This error reduction is clearly due to more accurate surface flux conditions provided by the ocean coupling. The operational GFDL model assumed fixed SSTs in time, while in the coupled the SSTs are allowed to change as a result of the ocean response to storm forcing.

Table 2. The GFDL operational and coupled hurricane-ocean model intensity forecast errors in the 1998 hurricane season. Average absolute errors (in hPa compared with observed values).

Time	Cases	Errors (hPa)		Impr. (%)
		Oper.	Coupled	
All cases				
12 h	98	12.29	9.32	24.2
24 h	91	17.03	12.51	26.6
36 h	85	19.73	13.64	30.9
48 h	75	21.59	15.23	29.4
60 h	69	23.42	17.47	25.4
72 h	62	23.87	18.81	21.2
Total	480	19.66	14.50	26.3
Hurricanes ($P_c < 980$ hPa)				
12 h	50	13.28	9.34	29.7
24 h	53	16.03	10.74	33.0
36 h	54	18.22	12.09	33.7
48 h	51	19.87	13.52	31.9
60 h	47	21.92	15.26	30.4
72 h	41	21.23	16.07	24.3
Total	296	18.42	12.84	30.5
Tropical Storms ($P_c > 980$ hPa)				
12 h	48	11.26	9.30	17.4
24 h	38	18.43	14.98	18.7
36 h	31	22.36	16.35	26.9
48 h	24	25.24	18.86	25.3
60 h	22	26.65	22.19	16.7
72 h	21	29.02	24.17	16.7
Total	184	22.16	17.64	20.3

3.2 The 1998 hurricane season

The coupled hurricane-ocean model has begun to be tested in near real time mode in the 1998 hurricane season. In total, 115 forecasts were performed (Tropical Storm Alex – 9, Hurricane Bonnie – 24, Hurricane Danielle – 18, Hurricane Earl – 7, Hurricane George – 42, Tropical Storm Hermine – 1, Hurricane Ivan – 4, Hurricane Jeanne – 10). The coupled model forecasts were made available to the National Hurricane Center via a dedicated Web site immediately after model integration. Error statistics for all cases every 12 hours are provided in Table 2. The mean absolute error of the central pressure forecasts is reduced by about 26 % compared to

the operational GFDL model. The largest improvements were achieved for the storms of hurricane (less than 980 hPa) intensity: 30.5 %. Among a total of 480 forecast verification times, the operational GFDL model overpredicted the storm intensity in 364 cases (average of 22.2 hPa) and underpredicted the intensity in 116 cases (average of 11.5 hPa). In the coupled model forecasts, the overprediction was reduced by 7.5 hPa but underprediction was only slightly increased by 2.5 hPa.

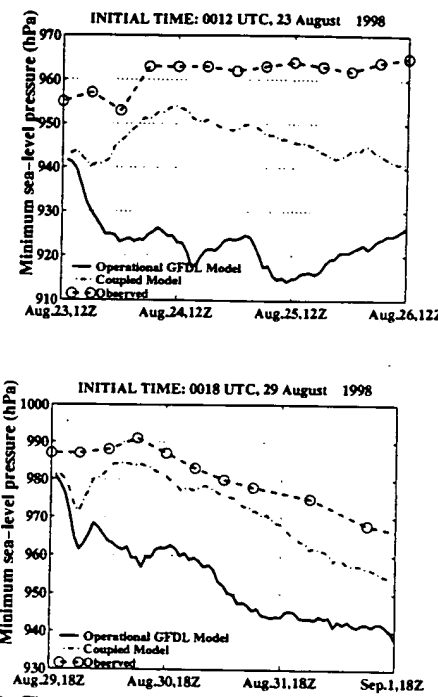


Figure 2: Time series of minimum sea-level pressure for operational forecast (solid line) and coupled model (dot-dashed line) compared to observed values (circles indicating values at every 6 hours) for the forecasts of Hurricane Bonnie (upper panel) and Danielle (lower panel)

Shown in Fig. 2 are the predicted 72 hour time series of the minimum sea-level pressure for one case each of Hurricanes Bonnie and Danielle. The observed values are also plotted. These examples represent some of the best cases and were obtained during important forecast periods. On August 23 Hurricane Bonnie was moving toward the U.S. east coast. The GFDL model track forecasts were generally fairly good. The model correctly predicted that the storm's forward speed would be reduced during that period. However, the intensity forecast indicated rapid storm intensification which resulted in large intensity overprediction (Fig. 2). That occurred because the operational model had responded to very warm water underneath the storm in the NCEP SST analysis. In the coupled model, the slow hurricane movement generated a large SST decrease below the storm. As a result, the storm intensity

forecasts were significantly improved. At initial time 1200 UTC August 23 shown in Fig. 2a, the coupled model correctly predicted that the hurricane would weaken by 1200 UTC August 24.

The GFDL model predicted movement of Hurricane Danielle at initial time 18 UTC August 29 was accurate, but the intensity forecast indicated again a significant overprediction. This was because the hurricane was moving very close to the cold wake generated by Hurricane Bonnie a few days before. Inclusion of this effect in the coupled model resulted in large improvement of the intensity forecast in this case (Fig. 2b). Fig. 3 shows the SST response to Hurricane Georges over the Gulf of Mexico simulated by the coupled model. Shallow mixed layer depths in the Gulf were conducive to substantial cooling of the sea surface along the storm track. The maximum cooling found to the right of the track reached about 3°C. The inclusion of this effect in the coupled model also led to substantial improvements of the hurricane intensity forecast.

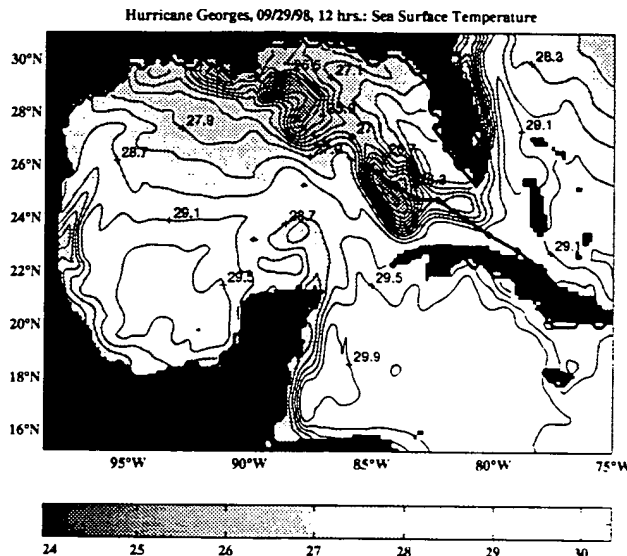


Figure 3. The SST distribution ($^{\circ}$ C) at 72 hours of the coupled model forecasts for Hurricane Georges (1200 UTC 26 September initial time). The observed track is shown by a solid line and forecasted track is a dashed line.

4. REMARKS

Evaluation of the coupled model forecasts for the 1998 hurricane season is in progress. In particular, the SST response in the coupled model is being compared with satellite AVHRR data where available. The ocean model initialization procedure is being carefully examined. For instance, the effects of replacing the NCEP 1° resolution SST analysis by

the 0.5° NESDIS SST data on the hurricane intensity prediction is investigated. Initialization of ocean fronts, such as the Gulf Stream in the North Atlantic and the Loop Current in the Gulf of Mexico needs to be addressed in the future work. In the next phase of improvements of the ocean model initialization, we aim to implement a new data assimilation scheme to include the initialization of frontal systems. Initialization of the coupled hurricane-ocean system must be improved as well. At present, the hurricane and ocean models are initialized independently. Moreover, the hurricane model does not take into account the cold wake underneath the storm during the vortex initialization. As a result, in some cases, significant overestimation of the initial central pressure was found which effected the coupled model forecasts.

ACKNOWLEDGMENTS

This work was supported by the National Science Foundation through grant ATM 9714412 and the U.S. Office of Naval Research through grant N000149610758. Programming assistance in establishing the automated forecast system from C. Rowley and S. Frolov is gratefully acknowledged. Computational support has been provided by the Department of Defense High Performance Computing Modernization Program at the Naval Oceanographic Office (NAVOCEANO) Major Shared Resource Center.

REFERENCES

- Bender, M.A., I. Ginis, 1998: Real case simulations of hurricane-ocean interaction using a high resolution coupled model: Effect on hurricane intensity. *Mon. Wea. Rev.*, Revised and resubmitted.
- Bender M.A., I. Ginis and Y. Kurihara, 1993: Numerical simulations of the tropical cyclone-ocean interaction with a high-resolution coupled model. *J. Geophys. Res.*, **98**, 23,245-23,263.
- Blumberg A.F., and G.L. Mellor, 1987: A description of a three-dimensional coastal ocean circulation model. *Three-Dimensional Coastal Ocean Models*, edited by N.S. Heaps, AGU, 1-16
- Ginis, I., M.A. Bender, and Y. Kurihara, 1997: Development of a coupled hurricane-ocean forecast system in the North Atlantic. *22nd Conf. on Hurricanes and Tropical Meteor.*, Ft. Collins, CO, Amer. Meteor. Soc., 443-444.
- Kurihara, Y., R.E. Tuleya, and M.A. Bender, 1998: The GFDL hurricane prediction system and its performance in the 1995 hurricane season, *Mon. Wea. Rev.*, **126**, 1306-1322.
- Mellor, G.L., 1996: User's guide for a three-dimensional, primitive equation, numerical ocean model. *Program in Atmospheric and Oceanic Sciences*, Princeton University, 35 pp.

Reference No. 7:

Holland, G.J., and Y. Wang, What Limits Tropical Cyclone Intensity, *Preprints of the 23rd Conference on Hurricanes and Tropical Meteorology*, January 10-15, 1999, Dallas, TX pp. 955-958 (1999).

23RD CONFERENCE ON HURRICANES AND TROPICAL METEOROLOGY

VOLUME II SESSIONS 8A-J16B

10-15 JANUARY 1999

DALLAS, TEXAS

SPONSORED BY
AMERICAN METEOROLOGICAL SOCIETY

Front Cover: Illustrations of the new NOAA-15 satellite Advanced Microwave Sounding Unit (AMSU) products during Hurricane Bonnie. The upper-level warm core of Bonnie is evident in the 55 GHz channel brightness temperatures (lower right). For comparison, the AVHRR IR-window image is also given (upper right). A vertical cross section (along 29N) of the thermal anomaly derived from AMSU-A multichannel temperature retrievals is shown in the bottom left (courtesy M. Goldberg, NOAA/NESDIS/ORA).

For more information on this study being conducted at UWISC-CIMSS under the support of ONR/NRL-MRY, refer to paper 4A.9 (page 182), entitled, "*Tropical Cyclone Warm Cores as Observed from the NOAA Polar Orbiting Satellite's New Advanced Microwave Sounding Unit,*" by Christopher S. Velden and K. F. Bruesky, CIMSS/University of Wisconsin, Madison, WI.

All Rights Reserved. No part of this publication may be reproduced or copied in any form or by any means – graphic, electronic, or mechanical, including photocopying, taping, or information storage and retrieval systems – without the prior written permission of the publisher. Contact AMS for permission pertaining to the overall collection. Authors retain their individual rights and should be contacted directly for permission to use their material separately. The manuscripts reproduced herein are unrefereed papers presented at the *23rd Conference on Hurricanes and Tropical Meteorology*. Their appearance in this collection does not constitute formal publication.

AMERICAN METEOROLOGICAL SOCIETY
45 BEACON STREET, BOSTON, MASSACHUSETTS USA 02108-3693

What Limits Tropical Cyclone Intensity?

Greg Holland¹ and Yuqing Wang
BMRC, Melbourne, Australia.

1. INTRODUCTION

As found empirically by several groups (Merrill 1988, DeMaria and Kaplan 1995, Evans 1993) the maximum intensity reached by tropical cyclones in all ocean basins are generally less than that which would be inferred from thermodynamic techniques (Emanuel 1986, Holland 1997) applied to climatological data. This raises the obvious question of what is limiting the majority of cyclones from reaching their climatological potential.

Tonkin et al. (1998) have shown that application of thermodynamic techniques to the conditions applying at the time of the cyclone development substantially narrows the differences between the maximum potential intensity and that achieved by the cyclone. It is also well known that local oceanic cooling associated with the passage of the cyclone can provide a major limit on the maximum intensity. And forecast lore has it that vertical wind shear is a major potential inhibitor of intensification to very severe systems.

We report on a study aimed at investigating the factors that may limit the intensification of tropical cyclones to their thermodynamic maximum potential. This abstract indicates some of the initial findings and the physical processes will be discussed in the presentation.

2. METHOD

We define tropical cyclone intensity by the pressure drop from the environment to the cyclone centre. Whilst this is somewhat arbitrary, central pressure is a reasonably conservative parameter, which does not suffer from the same degree of variability associated with maximum winds and the problem with of wind definition.

The environment is defined as everything external to the tropical cyclone core region. This includes

the underlying ocean, major cloud bands, the thermodynamic structure of the atmosphere in the outer cyclonic circulation (say, near the outermost closed isobar), imposed large-scale regimes (such as vertical windshear over the entire cyclone), and the multitude of systems at various atmospheric levels that undergo transient interactions with the tropical cyclone (such as upper troughs and mesoscale convective vortices).

Thermodynamic estimates of tropical cyclone intensity follow the method described by Holland (1997).

The numerical calculations use the model of Wang (1997). This is a triply tested, hydrostatic model in which the two internal grids follow the tropical cyclone. The resolution of the internal grid is 5 km. Moist processes are modelled by a full cloud physics package, with two phases of ice and a mixed ice-water process. Full details of this model may be found in Wang (1998 in preparation).

The method adopted has been to:

1. Undertake a series of comprehensive sensitivity experiments to indicate both the uncertainty arising from arbitrary selection of physical processes within the range of parameters quoted in the literature. This process indicated the degree of confidence in the following parametric studies, and potentially real uncertainties that may exist with actual tropical cyclones.

2. Utilise a series of experiments to investigate both the effects of imposed environments, such as vertical wind shear, and the associated physical processes.

The control model run used for comparison is initialised on an f-plane with no flow using the January-mean thermodynamic ocean and

¹Corresponding author address: Greg Holland, BMRC,
PO Box 1289K, Melbourne, Vic 3001 Australia
email g.holland@bom.gov.au

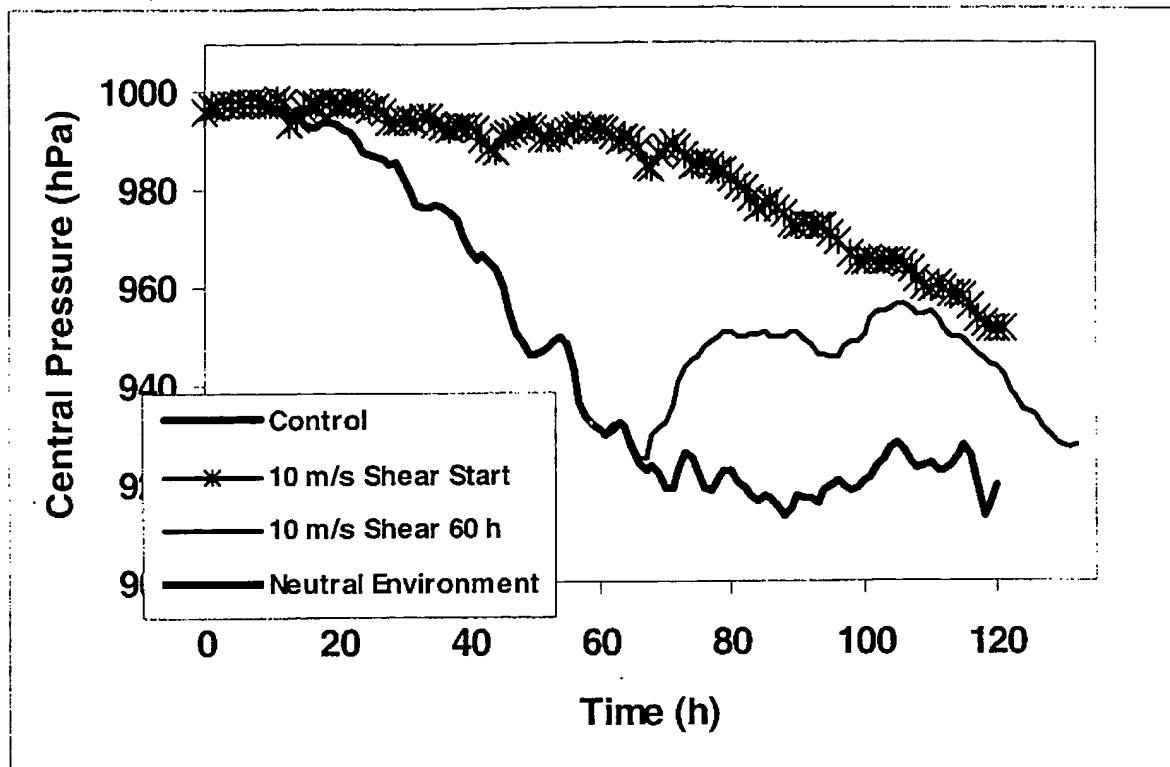


Figure 1. Intensification of the control cyclone with experiments with a thermodynamically neutral environment and with the imposition of vertical shear at the start and near the time of maximum intensity.

atmospheric conditions for Willis Island off the east coast of Australia.

3. PRELIMINARY RESULTS

We have noted considerable sensitivity to the details of the microphysical processes in the model clouds. For example, the defined fall speed for ice greatly effects the degree of stratiform clouds that develop. This also effects the degree of downdraft generation. Both of these processes can change the maximum intensity achieved by the model by up to 20%. The degree of surface heat exchange can markedly effect the temperature of the surface inflow layer, where air is moving rapidly towards lower pressure, expanding and cooling.

A feature that has appeared in many of our experiments is that development of substantial horizontal asymmetries or breakdown of the eye into smaller vortices is almost always associated with periods of weakening.

Rainbands are common features of tropical cyclones. Forecasting lore also indicates that they are associated with sustained intensification (the so-called "feeder band" rules). A recent study by May and Holland (1997) also has shown the generation of mid-level potential vorticity in such rainbands is quite high. This is sufficient to substantially effect the intensity if the vorticity can be advected to the core region. The apparent disagreement between these views and the finding of the modelling experiments has not yet been adequately explained.

Simpson et al. (1998) have described the potential impacts of transient changes to the thermodynamic environment that occur when a tropical cyclone develops in, for example, a large monsoon shear zone. In the case of Tropical Cyclone Oliver, this reduced the thermodynamic potential locally by 50% compared to the climatological maximum.

We are testing this effect by arbitrarily changing the thermodynamic characteristic of the environment. An extreme case is shown in Fig. 1,

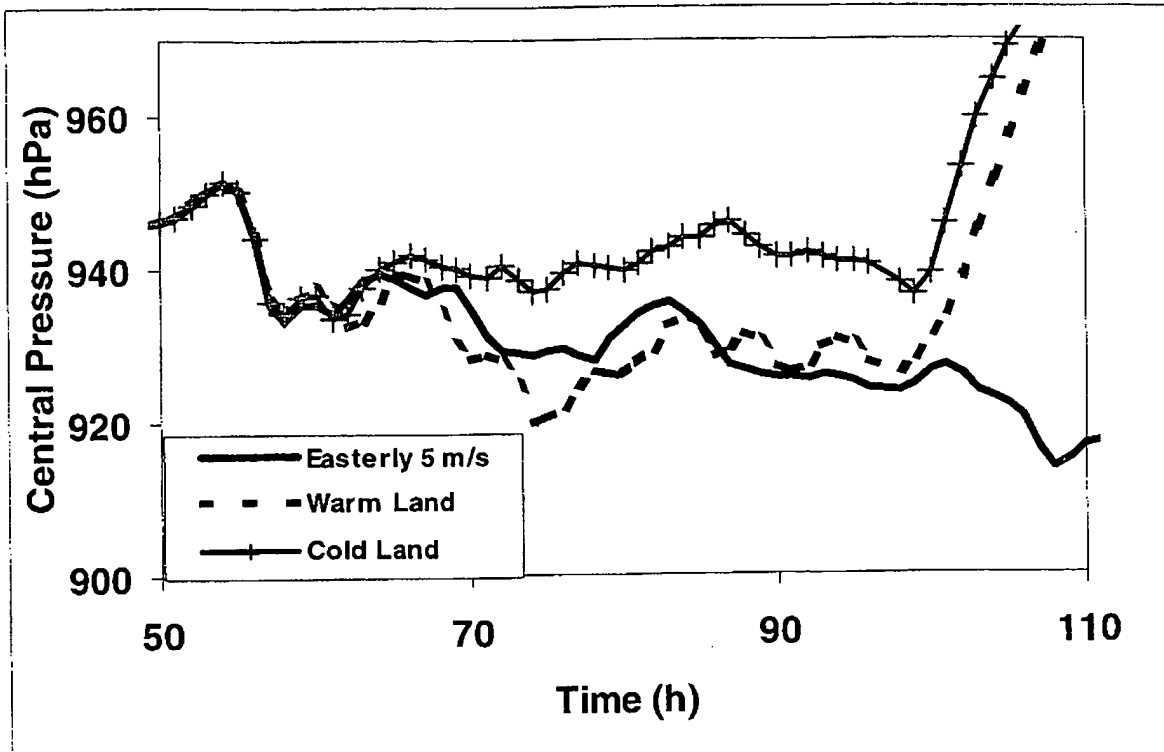


Figure 2. Effects on intensity of a landmass ahead of an eastward moving tropical cyclone in a uniform flow. Both the effects of a landmass held at the same as the SST, and a landmass that is cooled to 2K less than the SST are shown.

for an environment with an approximately moist adiabatic profile. In this case, the cyclone does not have any capacity for development.

Imposition of a linear vertical shear of 20 m/s between the surface and 100 hPa has different effects, depending on the intensity of the cyclone at the time the shear is applied (Fig. 1).

Imposing the shear when the cyclone is weak results in a much reduced initial intensification rate. Several days pass before the cyclone begins to intensify more rapidly. However, the cyclone eventually adjusts to the sheared environment and approaches its initial thermodynamic limit, as defined here by the control model.

When the same shear is applied close to the time of maximum intensity, the initial response is for the cyclone to become asymmetric and weaken. In this case the weakening appears to be associated with the asymmetric structure of the convection, rather than a direct shearing. However, after a period of weakening, the cyclone

adjusts to the shear and begins to intensify back to its thermodynamic limit.

We arrive at the preliminary conclusion that moderate amounts of shear effect the intensification rate, but cyclones will still reach their maximum potential intensity, albeit much more slowly.

Whilst it is well known that tropical cyclones will weaken if they move over a major landmass, it is of some interest to examine the effects of a landmass before the cyclone makes landfall (Fig. 2). The land in this case is flat and at sea level, but its surface temperature is set equal to the SST (warm land) or 2K cooler (cold land).

It is remarkable that the presence of cold land weakens the cyclone up to 35 h before it actually moves over land. This weakening is sustained and the cyclone does not recover, though there is evidence of a small intensification near land. The warm land has a much smaller effect, though it

does lead to a short period at maximum intensity approximately 24 hour before landfall.

We shall describe the associated processes in the presentation. The weakening for the cold land case appears to be associated with the inhibition of convection over the land and the resulting development of strong asymmetries in the cyclone.

4. Conclusions

A series of sensitivity experiments with an advanced numerical model are being made to examine the effects of various imposed condition on tropical cyclone intensification. Also being examined are the associated physical processes.

The findings reported here indicate that moderate amounts of vertical shear effect the rate of intensification of tropical cyclones. Shear does not effect the maximum intensity that can be achieved. Any major convective asymmetry in the cyclone appears to reduce the maximum intensity that can be achieved. However, in the absence of a maintenance mechanism, the cyclone eventually returns to an approximately symmetric shape and its thermodynamic intensity limit.

An interesting finding is that the presence of land, even several hundred km away from the cyclone centre can have a significant influence on the maximum intensity that can be reached.

Acknowledgement: Partial funding for this research has been provided by the Office of Naval Research under grant N-00014-94-1-0493.

REFERENCES

- Black, P.G. and G.J. Holland, 1995: The Boundary Layer of Tropical Cyclone Kerry (1979). *Mon. Wea. Rev.*, **123**, 2007-2028.
- Byers, H.R., 1944: *General Meteorology*. McGraw-Hill Book Company, New York, London.
- DeMaria, M. and J. Kaplan, 1995: Sea surface temperature and the maximum intensity of Atlantic tropical cyclones. *J. Climate*, **7**, 1324-1334.
- Emanuel, K.A., 1986: An air-sea interaction theory for tropical cyclones. Part 1: Steady-state maintenance. *J. Atmos. Sci.*, **43**, 585-604.
- Evans, J.L., 1993: Sensitivity of tropical cyclone intensity to sea surface temperature. *J. Climate*, **6**, 1133-1140.
- Holland, G.J., 1997: The Maximum potential intensity of tropical cyclones. *J. Atmos. Sci.*, **54**, 2519-2541.
- May, P.T. and G.J. Holland, 1997: The role potential vorticity generation in tropical cyclone rainbands. *Mon. Wea. Rev.* (Submitted).
- Simpson, J., E.A. Ritchie, G.J. Holland, J. Halverson and S. Stewart, 1997: Mesoscale interactions in tropical cyclogenesis. *Mon. Wea. Rev.*, **125**, 2643-2661.
- Merrill, R.T., 1988: Environmental influences on hurricane intensification. *J. Atmos. Sci.*, **45**, 1678-1687.
- Merrill, R.T., 1993: Tropical Cyclone Structure. *Chapter 2 of the Global Guide to Tropical cyclone Forecasting WMO/TD-560* (G.J. Holland, ed.), World Meteorological Organization, Geneva, pp2.1.1-2.60.
- Simpson, J., E.A. Ritchie, G.J. Holland, J. Halverson and S. Stewart, 1997: Mesoscale interactions in tropical cyclone genesis. *Mon. Wea. Rev.*, (In Press).
- Tonkin, H., 1997: Investigating Thermodynamic Models of Tropical Cyclone Intensity. *MSc Thesis*, Climatic Impacts Centre, Macquarie University, Sydney, Australia.
- Wang, Y., 1995: On an inverse balance equation in sigma-coordinates for model initialisation. *Mon. Wea. Rev.*, **123**, 482-488.
- Wang, Y., 1997: A triple-nested tropical cyclone model. *Aust. Meteor. Mag.*, (Submitted).

Reference No. 8:

Holland, G.J. and Y. Wang, Limitations on Hurricane Intensity, Session 1A of the 24th Conference on Hurricanes and Tropical Meteorology Fort Lauderdale, FL, Paper 1A.5 (Figure 2-12 of this report provided courtesy of senior author) (2000).

of 100

24TH CONFERENCE ON HURRICANES AND TROPICAL METEOROLOGY

29 MAY-2 JUNE 2000

FORT LAUDERDALE, FL

SPONSORED BY
AMERICAN METEOROLOGICAL SOCIETY

Front Cover: Progress in hurricane intensity modeling. The left panels show the evolution of the maximum wind speeds in Hurricanes Gert and Bret of 1999. In each panel, the green curves show the maximum winds estimated from observations, while the blue curves show "hindcasts" of the intensity using a very simple coupled ocean-atmosphere model, as described in Paper 6A.5 (page 236), entitled, "*Forecast Skill of a Simplified Hurricane Intensity Prediction Model,*" by Kerry A. Emanuel, MIT, Cambridge, MA; and E. Rappaport. The underprediction of Hurricane Bret may have been related to Bret's passage over anomalously deep, warm water, as illustrated by the satellite-derived pre-storm distribution of sea surface temperature shown at lower right and discussed in Papers J1.3 (page J5), entitled, "*Role of the Upper Ocean Structure on the Intensification of Hurricane Bret from Satellite Altimetry*" by Gustavo J. Goni, NOAA/AOML, Miami, FL; and L. K. Shay, P. G. Black, S. D. Jacob, T. M. Cook, J. J. Cione, and E. Uhlhorn and paper J1.4 (page J7), entitled, "*Hurricane Intensity Change Modulated by Air-sea Interaction Effects Based on Unique Airborne Measurements During the 1998-99 Hurricane Seasons*", by Peter G. Black, NOAA/AOML/HRD, Miami, FL; and E. W. Uhlhorn, J. J. Cione, G. J. Goni, L. K. Shay, S. D. Jacob, E. J. Walsh, and E. A. D'Asaro and The upper right panel shows a an enhanced color satellite image of Hurricane Gert.

The cover image was provided by Kerry A. Emanuel, MIT, Cambridge, MA, with sponsorship from the Center for Global Change Science, MIT, Cambridge, MA.

All Rights Reserved. No part of this publication may be reproduced or copied in any form or by any means – graphic, electronic, or mechanical, including photocopying, taping, or information storage and retrieval systems – without the prior written permission of the publisher. Contact AMS for permission pertaining to the overall collection. Authors retain their individual rights and should be contacted directly for permission to use their material separately. The manuscripts reproduced herein are unrefereed papers presented at the **24th Conference on Hurricanes and Tropical Meteorology**. Their appearance in this collection does not constitute formal publication.

AMERICAN METEOROLOGICAL SOCIETY
45 BEACON STREET, BOSTON, MASSACHUSETTS USA 02108-3693

TABLE OF CONTENTS

24TH CONFERENCE ON HURRICANES AND TROPICAL METEOROLOGY

PAGE

SESSION 1A: TROPICAL CYCLONE INTENSITY CHANGE THEORY I

- 1 1A.1 SST TIME SERIES DIRECTLY UNDER TROPICAL CYCLONES: OBSERVATIONS AND IMPLICATIONS. Joseph J. Cione, NOAA/AOML/HRD, Miami, FL; and P. Molina, J. Kaplan, and P. G. Black
- 585 1A.2 ON THE RAPID INTENSIFICATION OF HURRICANE OPAL (1995) OVER THE GULF OF MEXICO. V. Mohan Karyampudi, Univ. of Maryland, College Park, MD; and E. B. Rodgers, H. F. Pierce, and J. Weinman
- * 1A.3 MINIMUM POTENTIAL PRESSURES OF TROPICAL CYCLONES OVER THE EASTERN NORTH PACIFIC OCEAN FROM THE NCEP/NCAR REANALYSES. Jay S. Hobgood, Ohio State Univ., Columbus, OH
- 3 1A.4 MICROWAVE SST CORRELATION WITH CYCLONE INTENSITY. Chelle Gentemann, Remote Sensing Systems, Santa Rosa, CA; and D. Smith and F. Wentz
- * 1A.5 LIMITATIONS ON HURRICANE INTENSITY. Greg J. Holland, BMRC, Melbourne, Vic, Australia; and Y. Wang
- 5 1A.6 EFFECTS OF VERTICAL SHEAR ON THE STRUCTURE AND INTENSITY OF HURRICANES. William M. Frank, Penn State Univ., University Park, PA; and E. A. Ritchie
- 7 1A.7 A CLIMATOLOGY OF HURRICANE MAXIMUM POTENTIAL INTENSITY IN THE ATLANTIC BASIN. Christopher C. Hennon, Ohio State Univ., Columbus, OH

SESSION 1B: TROPICAL WAVES AND INSTABILITIES I [This Session will be Dedicated to the Memory of Dr. Yoshikazu Hayashi, GFDL]

- 9 1B.1 WATER VAPOR ANOMOLY TROPICAL WAVE TRACING. Paul E. Roundy, Penn State Univ., University Park, PA
- 11 1B.2 THE ENERGETICS OF THE AFRICAN EASTERLY WAVE LIFE CYCLE: A CASE STUDY. Lourdes B. Avilés, Univ. of Illinois, Urbana, IL
- 13 1B.3 ROLE OF EASTERLY WAVE IN THE MAINTENANCE OF THE EASTERLY JET. Rosana Nieto Ferreira, NASA/GSFC and USRA, Greenbelt, MD; and M. Suarez and J. T. Bacmeister
- * 1B.4 THE DYNAMICS OF THE AFRICAN EASTERLY JET. PART II: GCM SIMULATIONS. Julio T. Bacmeister, USRA, Seabrook, MD; and M. J. Suarez and R. N. Ferreira
- 15 1B.5 SPACE-TIME SPECTRA OF WESTWARD-PROPAGATING SYNOPTIC-SCALE DISTURBANCES IN THE ITCZ. Guojun Gu, Univ. of Miami/RSMAS, Miami, FL
- * 1B.6 POTENTIAL VORTICITY STRUCTURE AND EVOLUTION IN AFRICAN EASTERLY WAVES. Michael C. Morgan, Univ. of Wisconsin, Madison, WI; and G. A. Postel
- 17 1B.7 IDEALIZED MODELING OF TROPICAL EASTERLY DISTURBANCES. Anantha R. Aiyyer, SUNY, Albany, NY; and J. Molinari

SESSION 1C: INTERANNUAL VARIATIONS OF TROPICAL CYCLONES

- * 1C.1 EXTENDED RANGE FORECASTING OF NW PACIFIC AND SW PACIFIC LANDFALLING TROPICAL CYCLONES. Paul Rockett, Univ. College London, Dorking, Surrey, UK; and M. A. Saunders
- 19 1C.2 LOCAL ENVIRONMENTAL CONDITIONS RELATED TO SEASONAL HURRICANE ACTIVITY IN THE NE PACIFIC BASIN. Jennifer M. Collins, Univ. College London, Dorking, Surrey, UK
- 21 1C.3 INTERANNUAL AND DECADAL VARIABILITY OF TROPICAL CYCLONE ACTIVITY OVER THE CENTRAL NORTH PACIFIC. Pao-Shin Chu, Univ. of Hawaii, Honolulu, HI; and J. Clark and B. Lin

AUTHOR INDEX

24TH CONFERENCE ON HURRICANES AND TROPICAL METEOROLOGY

<u>PAPER #</u>	<u>PAGE</u>	<u>PAPER #</u>	<u>PAGE</u>		
V(Continued)			W(Continued)		
Vazquez, J. L.	P1.10	155	Webster, P. J.	16B.8	*
Velden, C. S.	5A.5	126	Webster, P. J.	J2.4	*
Velden, C. S.	P1.3	145	Webster, P. J.	J2.5	*
Velden, C. S.	6A.7	240	Webster, P. J.	J2.6	*
Velden, C. S.	7A.4	256	Webster, P. J.	J4.7	*
Velden, C. S.	7A.5	258	Weindl, H.	P1.36	185
Velden, C. S.	14B.2	*	Weinman, J.	1A.2	585
Velden, C. S.	15A.6	488	Weisberg, R. H.	J8.5	J64
Velden, C. S.	15A.8	492	Wells, M. G.	J3.7	J27
Vijaya Kumar, T. S. V.	J6.5	J47	Weng, C.-H.	J4.4	J34
Vizy, E. K.	11B.3	366	Weng, F.	14B.1	460
Vladimirov, V. A.	13A.8	420	Wentz, F.	1A.4	3
Vollaro, D.	6B.1	242	Wentz, F.	15A.7	490
Voner Haar, T. H.	15A.4	484	Wheeler, M.	2B.5	47
Vázquez, J. L.	4B.6	116	Wheeler, M.	2B.6	*
			White, S. R.	P1.27	175
			Whitehead, D.	17A.5	*
W			Wienman, J.	16B.7	537
Wainscoat, R.	12C.7	406	Willemet, J.-M.	13B.4	425
Walsh, E. J.	10A.2	327	Williams, E.	5B.7	141
Walsh, E. J.	J1.1	J1	Williams, K. F.	17A.7	559
Walsh, E. J.	J1.4	J7	Williams, R. T.	2B.1	41
Walsh, K. J. E.	14C.1	470	Williford, C. E.	J6.5	J47
Walsh, K. J. E.	14C.4	476	Willoughby, H. E.	3B.5	83
Walters, J.	10A.7	590	Willoughby, H. E.	P1.37	187
Wang, B.	3B.4	81	Willoughby, H. E.	13A.5	416
Wang, B.	J4.3	J32	Willoughby, H. E.	17A.6	557
Wang, C.	J6.2	J42	Wolff, D. B.	9A.1	296
Wang, H.	13B.1	421	Wood, E. C.	P1.14	159
Wang, J.	8A.5	276	Wood, S. A.	11A.6	360
Wang, J.	17C.2	575	Wright, C. W.	10A.2	327
Wang, J.	17C.4	579	Wright, C. W.	J1.1	J1
Wang, S.	J7.3	J51	Wright, J. E.	P1.33	181
Wang, T.-A.	8A.6	278	Wroe, D. R.	J8.3	J60
Wang, Y.	1A.5	*	Wu, C.-C.	8A.2	272
Wang, Y.	P1.53	*	Wu, C.-C.	13B.3	423
Wang, Y.	12A.2	*	Wu, K.	P1.68	224
Wang, Y.	17C.1	573	Wu, L.	3B.4	81
Wang, Y.	J2.3	J19	Wu, M. C.	4B.3	110
Warner, T. T.	13C.4	439	Wu, R.	J4.3	J32
Weber, H. C.	12A.6	378			
Webster, P. J.	3C.3	*	X		
Webster, P. J.	4B.2	*	Xie, L.	P1.68	224
Webster, P. J.	P1.29	*	Xie, S.-P.	13C.5	440
Webster, P. J.	P1.51	*	Xu, J.	12C.1	396
Webster, P. J.	P1.57	208	Xu, J.	17C.1	573
Webster, P. J.	11B.6	*	Xu, M.	13C.4	439
Webster, P. J.	12C.3	400	Xu, X.	P1.13	157
Webster, P. J.	13C.7	444			

24th Conference on Hurricanes and Tropical Meteorology

1A.5

LIMITATIONS ON HURRICANE INTENSITY

Greg J. Holland and Yuqing Wang. BMRC, Melbourne, Australia

Previous studies have shown that thermodynamic estimates based on long - term mean conditions provided an excellent upper bound on tropical cyclone intensity, the so-called Maximum Potential Intensity. However, it is also well known that most tropical cyclones do not reach this upper bound. We discuss our progress in identifying the processes that can limit the cyclone intensification and prevent cyclones reaching the maximum intensity.

Using a series of numerical experiments, we show how fine-scale details of the convective and mesoscale structure of a tropical cyclone can have a marked impact on the cyclone intensification. We also examine the effects of cyclone movement and proximity to land and oceanic thermal anomalies. This research confirms our earlier findings that most processes act to inhibit, rather than enhance the cyclone intensification potential.

[AMS Home Page](#)

Reference No. 9:

Schade, L.R., and K.A. Emanuel, The Ocean's Effect On The Intensity Of Tropical Cyclones: Results From A Simple Coupled Atmosphere-Ocean Model, *Journal of the Atmospheric Sciences*, Vol. 56, pp. 642-651 (1999).

The Ocean's Effect on the Intensity of Tropical Cyclones: Results from a Simple Coupled Atmosphere–Ocean Model

LARS R. SCHADE

Meteorologisches Institut der Universität München, Munich, Germany

KERRY A. EMANUEL

Program in Atmospheres, Oceans, and Climate, Massachusetts Institute of Technology, Cambridge, Massachusetts

(Manuscript received 24 November 1997, in final form 21 April 1998)

ABSTRACT

A coupled hurricane–ocean model was constructed from an axisymmetric hurricane model and a three-layer ocean model. If the hurricane moves at constant speed across the ocean a statistically steady state (in a reference frame moving with the storm) is reached after a few days of simulation time. The steady-state intensity of the hurricane is strongly affected by the interaction with the ocean. This interaction with the ocean can be described as a negative feedback effect on the hurricane's intensity and is called "SST feedback." A large set of numerical experiments was performed with the coupled model to deduce systematically the dependence of the amplitude of the SST feedback effect on a set of model parameters.

In the coupled model the SST feedback effect can reduce the hurricane's intensity by more than 50%. Only in cases of rapidly moving storms over deep oceanic mixed layers is the SST feedback effect of minor importance. These results cast a new light on the role of the ocean in limiting hurricane intensity.

1. Introduction

Hurricanes¹ form exclusively over the tropical oceans and rapidly disintegrate when they make landfall. This is primarily due to the much-reduced surface heat fluxes over land. Since the surface fluxes peak sharply just outside and under the eyewall, a hurricane effectively "feels" the land when the eye of the storm moves onshore even though a large part of the storm's circulation may have been over land much earlier. This becomes most striking when a hurricane moves parallel to the shore line in close vicinity to land, as often happens with recurving storms along the U.S. east coast (e.g., Hurricanes Emily, 1993, and Danny, 1997).

The fundamental role of the surface heat fluxes (foremost that of latent heat) as the energy source of hurricanes has been recognized for a long time (e.g., Riehl 1950; Kleinschmidt 1951). It has also been known since the 1960s that hurricanes leave a wake of cold surface

water behind them (e.g., Leipper 1967) that results from rapid turbulent entrainment of cold water into the oceanic mixed layer. Nevertheless, the effect of this cooling on the intensity of hurricanes has received surprisingly little attention. In numerical hurricane models, the ocean was typically treated as a constant sea surface temperature (SST) boundary condition and the effect of the chosen SST field on hurricane intensity was investigated (e.g., Ooyama 1969). Similarly, in numerical ocean models, the hurricane wind field was specified and the oceanic response to the specified hurricane forcing was investigated (e.g., Price 1981). In both approaches one part of the coupled atmosphere–ocean system is treated as active and the other part as passive, such that any feedback effects are excluded a priori.

The first numerical simulations of the coupled hurricane–ocean system were performed with axisymmetric hurricane and ocean models neglecting the hurricane movement. Very limited computer power dictated a coarse horizontal resolution resulting in only weak model storms. From such model simulations Chang and Anthes (1979) concluded that "appreciable weakening of a hurricane due to the cooling of the oceanic surface will not occur if it is translating at typical speed." The fact that their model storm was only very little affected by a rather strong oceanic cooling is likely due to a combination of several problems including their convective parameterization (based on moisture conver-

Corresponding author address: Dr. Lars R. Schade, Institut für Meteorologie der Universität München, Theresienstr. 37, D-80333 Munich, Germany.
E-mail: schade@lrz.uni-muenchen.de

¹ The term "hurricane" is used loosely in this paper to refer to tropical cyclones in general.

gence), the short integration period of only 24 h, and the aforementioned problems of coarse resolution and thus weak storms. Sutyrin et al. (1979) performed simulations with a coupled model of the oceanic and atmospheric boundary layers and concluded that the "interaction is so strong that the integral heat and moisture fluxes from the ocean into the atmosphere may change significantly within a few hours and influence the intensity of the tropical cyclone." Sutyrin and Khain (1984) coupled an axisymmetric hurricane model to a 3D ocean model and were the first to simulate the effect of the storm movement on the intensity of the storm. They showed that smaller storm translation speeds and smaller initial oceanic mixed layer depths lead to a stronger negative feedback effect of the ocean on the intensity of the hurricane. A fully three-dimensional coupled model was presented by Khain and Ginis (1991) and used to study the effect of the interaction with the ocean on the storm track. Bender et al. (1993) published results from simulations with a very high resolution fully three-dimensional coupled hurricane-ocean model confirming many of the earlier results. While these coupled model simulations have revealed some of the basic aspects of the oceanic feedback effect on hurricane intensity, this feedback has not yet been investigated systematically. Many scientists and forecasters therefore believe that the SST feedback need not be considered to first order, much in the spirit of the early results of Chang and Anthes. How commonplace this belief still is can be seen in a recent portrait of the state of tropical cyclone research by the World Meteorological Organization (Foley et al. 1995). In this paper we hope to suggest a new and different perspective on the effect of the ocean on hurricane intensity.

2. Goal and approach

The goal of this investigation is to understand and quantify the effect of the ocean on the intensity of tropical cyclones. The effects can be categorized into two classes: noninteractive effects in which the ocean is passive, and interactive or feedback effects. The first class of effects can be investigated by quantifying the sensitivity of a hurricane model to its lower boundary condition, a constant SST field. Physically, these effects are primarily caused by the dependence of the surface fluxes on the saturation vapor pressure at the SST. In contrast, investigation of the second class of effects requires a coupled hurricane-ocean model. Ocean dynamics now come into play in addition to the thermodynamics at the atmosphere-ocean interface.

The foci of this paper are the interactive effects of the ocean on hurricane intensity. The noninteractive effects are only briefly addressed in section 3b(1). A quantitative measure of the ocean's interactive effects on a hurricane's intensity is the SST feedback factor F_{SST} :

$$F_{\text{SST}} = \frac{\Delta p}{\Delta p|_{\text{SST}}} - 1, \quad (1)$$

where Δp is the pressure depression in the eye of the storm, that is, the difference between the background surface pressure far away from the storm and the minimum central pressure in the eye. Here Δp serves as a measure of storm intensity. The subscript SST refers to the pressure depression realized with a fixed sea surface temperature, that is, without any feedback. The factor F_{SST} is always negative because a reduction of the SST due to the storm diminishes the storm's intensity; F_{SST} therefore must be in the range $[-1; 0]$. An SST feedback factor of $F_{\text{SST}} = -0.3$, for example, means that the storm's intensity as described by the pressure depression is reduced by 30% due to the SST feedback effect. The central question of this paper is, *How does the SST feedback factor depend on the parameters of the coupled hurricane-ocean system?*

In a complex natural setting, F_{SST} depends not only on a number of environmental parameters but also on the history of the storm. To exclude such a dependence on time only mature storms shall be considered; that is, it is assumed that the coupled hurricane-ocean system has had enough time to settle into an equilibrium state. This state is characterized by a statistical steadiness of all variables in a frame of reference moving with the storm. The SST feedback factor of the mature hurricane-ocean system no longer depends on time but only on the environment of the hurricane-ocean system.

To investigate the parameter dependence of F_{SST} , a coupled hurricane-ocean model was constructed from the axisymmetric hurricane model of Emanuel (1989) and the 3D ocean model of Cooper and Thompson (1989). This choice of models was made to make possible a large number of simulations and thus to allow for a systematic exploration of the parameter space. The coupled model is a process model rather than a forecast model. Its main limitations are the lack of detailed cloud microphysics and the restriction of axisymmetry in the atmosphere. Nevertheless, it is expected that the basic features of the SST feedback effect are reasonably well represented in this simple coupled model.

The approach can be summarized as follows. First, comprehensive sensitivity tests with the uncoupled hurricane model were performed to select a set of environmental parameters that are hypothesized to be relevant to the SST feedback effect. In the range of observed values of these parameters the parameter space was then sampled systematically with the coupled model. Finally, a statistical regression was performed to deduce an analytical expression for the dependence of the SST feedback factor on the environmental parameters.

3. Models

A coupled hurricane-ocean model was constructed from two independently developed and tested models,

namely, the axisymmetric hurricane model of Emanuel (1989) and the four-layer ocean model of Cooper and Thompson (1989). As both models have been described in detail elsewhere, the model equations are not derived here again. Instead, both models are briefly introduced from a physical perspective describing the principal physical processes and balances in the models. Those readers interested in the technical details are referred to the original publications. While the original hurricane model is expressed in dimensionless variables, an analogous set of dimensional equations was used to ease the coupling to the dimensional ocean model. The derivation of this set of dimensional model equations is given in Schade (1994). Finally, the coupling procedure by which information is exchanged between the two submodels is described at the end of this section.

a. Hurricane model

The hurricane model is an axisymmetric model in gradient-wind and hydrostatic balance. It thus belongs to the "models of the first phase" as defined by Ooyama (1982). Since the present application is restricted to the mature stage of tropical cyclones, the use of a balanced model is justified. The model atmosphere consists of three layers: a boundary layer and two tropospheric layers. In the radial direction, the model uses angular momentum coordinates. Two main advantages arise from this choice of coordinate system. First, the radial resolution in physical space is high in regions where the radial gradient of angular momentum is large. Thus a domain of 2000-km radius can be represented with only 48 radial nodes and yet achieve a resolution of 3–10 km grid spacing in the region of main interest under the eyewall. Second, the slantwise convection in the eyewall of a tropical cyclone, which is typically tilted at an angle of 30°–60°, becomes upright in the framework of angular momentum coordinates and thus easy to represent. At this resolution a time step of 1 min is required for numerical stability.

The turbulent exchange of momentum between atmosphere and ocean is parameterized using the bulk aerodynamic drag law with a wind speed-dependent drag coefficient. Aside from the effect of radial diffusion, angular momentum is strictly conserved in the interior of the model atmosphere. Since the air flowing in toward the eye at low levels rotates cyclonically, surface friction constantly removes cyclonic angular momentum from the model atmosphere. The angular momentum budget of the model can therefore never settle into a true steady state. Nevertheless, a steady state can be reached at low levels if the radial advection of high angular momentum is balanced by the frictional loss to the lower boundary. The permanent transfer of angular momentum to the ocean is reflected in the ever-growing anticyclone in the upper-atmospheric layer. In angular momentum coordinates, this simply means that the coordinate surfaces are advected outward by the

mean radial flow to ever larger radii. While this is clearly unrealistic, it is an artifact of the axisymmetry that does not allow for a mean vertical shear in the troposphere and thus for a flow through the upper anticyclone. In nature, such shear causes a ventilation of the upper-tropospheric anticyclone and a downstream wake of air with low potential vorticity (e.g., Wu and Emanuel 1993). Since there is no vertical diffusion of momentum in the model a steady state can be reached in the lower troposphere in spite of the ever-growing anticyclone aloft.

Similar to momentum, heat is transferred turbulently between atmosphere and ocean and again the bulk aerodynamic drag law is used to parameterize this transfer. In the interior of the atmosphere, two nonconservative processes are included in the model. First, the release of latent heat due to phase changes of water is treated implicitly by using moist entropy as a combined temperature and humidity variable. Second, radiative cooling is crudely parameterized as a Newtonian relaxation back to the initial convectively neutral sounding. Unlike momentum, the moist entropy in the different layers is strongly coupled through convection. As soon as surface fluxes or radiative cooling render the stratification at a grid point unstable, a convective mass flux is triggered that acts to return the profile back to neutrality. In the steady state, surface fluxes, radiation, and convection balance advection of moist entropy. Though radiation plays a minor role for short integration periods and is often neglected in hurricane models, it is a fundamental part of the overall heat balance and a prerequisite for reaching a steady state.

The model is initialized with a marginal tropical storm and a convectively neutral stratification. The constraint of convective neutrality implies that the initial atmospheric sounding is a function of the initial SST and of the initial relative humidity in the boundary layer (\mathcal{H}). Physically this initial condition corresponds to a situation where the unperturbed atmosphere has had enough time to adjust to the ocean surface below it. Typically, the initial vortex first spins down slightly owing to friction and convective downdrafts, before the core becomes saturated and intensification begins. The storm then rapidly develops over the next 2–4 days and finally settles into a statistically steady state. Such a typical development is shown in Fig. 1.

b. Sensitivity tests

Many parameters need to be set for a numerical model even if it is as simple as the hurricane model used here. Few of these parameters have a direct physical meaning and can be considered known. The majority of the parameters, such as the bulk drag coefficient, is only known to fall into a certain range of values. Again, other parameters have no direct physical meaning, for example, the length of the time step in the model, but nevertheless may have a strong influence on the model

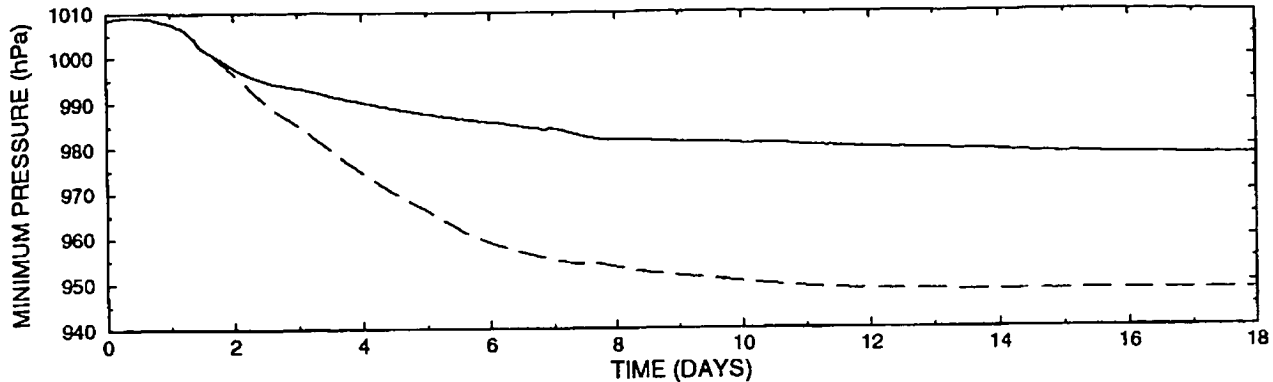


FIG. 1. Time series of the minimum central pressure. The solid line marks the results of a coupled integration while the dashed line is from an identical integration with constant SST. The following dimensional parameters were used: $h_o = 40$ m, $u_r = 6$ m s $^{-1}$, $\Delta p_{\text{sst}} = 65$ hPa, $\eta = 0.8$, $f_o = 5 \times 10^{-5}$ s $^{-1}$, $T = 8 \times 10^{-1}$ °C m $^{-1}$, and $\mathcal{H} = 84\%$. The value of Δp_{sst} results from SST = 29°C and $T_{\text{mp}} = -68^\circ\text{C}$ (and $\mathcal{H} = 84\%$).

results. Therefore the sensitivity of the model results to *all* input parameters was tested to discover physical sensitivities of interest and erroneous sensitivities of concern. For sake of conciseness only those results of the sensitivity tests are reported here that are of physical interest or that highlight weaknesses of the model. Put differently, the model results are insensitive to all parameters not mentioned below.

In each set of sensitivity experiments, the sensitivity of the steady-state central pressure to changes in only a single parameter was tested over a range of values considered realistic. All the other parameters were held fixed at their default values. It should be noted, though, that changes in SST and changes in \mathcal{H} imply changes in the initial atmospheric temperature because the atmosphere is assumed to be convectively neutral at the initial time.

1) SEA SURFACE TEMPERATURE

When the hurricane model is run uncoupled, the SST is constant in time and horizontally uniform. Higher SSTs lead to more intense storms as expected and pre-

dicted, for example, by the Carnot theory for hurricanes (Emanuel 1988). A sensitivity of about -6 hPa/K was found (Fig. 2). The default SST is 29°C.

This sensitivity constitutes the noninteractive effect of the ocean on the hurricane's intensity.

2) RELATIVE HUMIDITY

In the initial unperturbed model atmosphere, the relative humidity in the boundary layer must be specified. Lower relative humidity leads to stronger storms. While it may seem counterintuitive that a dryer boundary layer gives rise to a more intense moist convective storm the reason for this behavior is quite simple: a dryer boundary layer features a stronger thermodynamic disequilibrium at the sea surface. This becomes most apparent in the extreme scenario of $\mathcal{H} = 100\%$ in which the latent heat flux goes to zero. The sensitivity is about 4 hPa/% as shown in Fig. 3. The default relative humidity is 80%.

3) INITIAL CONDITIONS

The final steady state is insensitive to the specification of the initial vortex. Such a lack of sensitivity is gen-

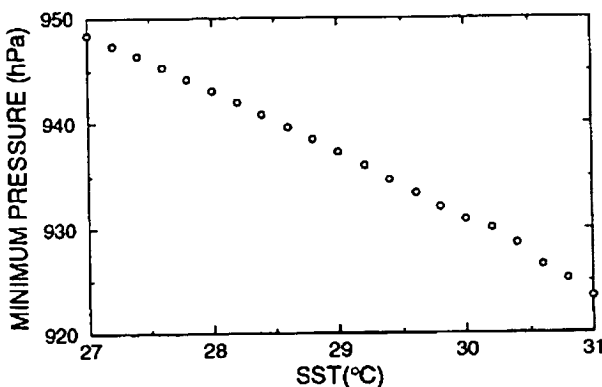


FIG. 2. Sensitivity of the steady-state central pressure to the SST.

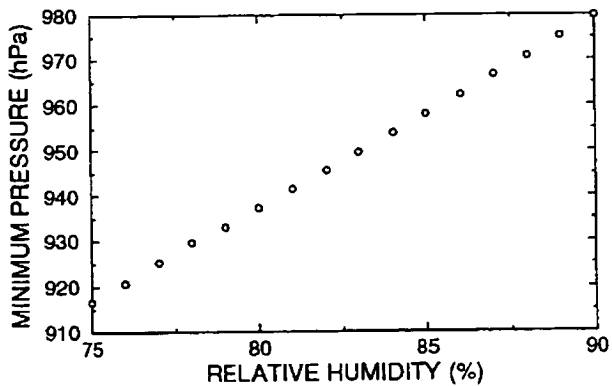


FIG. 3. Sensitivity of the steady-state central pressure to the relative humidity.

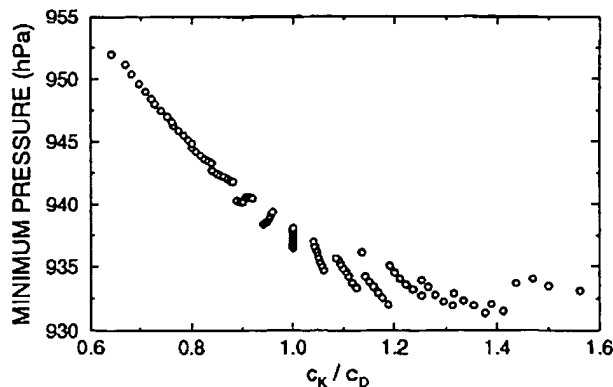


FIG. 4. Sensitivity of the steady-state central pressure to the ratio of the transfer coefficient of heat to that of momentum.

erally very desirable in models that are run to an equilibrium state. Yet in nature, hurricanes of very different sizes have been observed and it is important to investigate how the feedback effect in the coupled model changes with storm size. Our expectation that the final size of the model storm depends on the size of the initial vortex turned out to be wrong and the storm size had to be specified rather artificially in the coupled experiments as described in section 3d.

The default storm has maximum winds of 52 m s^{-1} at a radius of 40 km. Gale force winds extend to a radius of 150 km.

4) TRANSFER COEFFICIENTS

In the default experiment, the transfer coefficients for momentum and heat in the bulk aerodynamical formulas are identical and the storm intensity is insensitive to the choice of value. But a strong dependence on the ratio of the transfer coefficient for heat to that for momentum was found and is displayed in Fig. 4. Ooyama (1969) had already qualitatively described this effect and it is discussed in detail in Emanuel (1995). It is mentioned here because the physics and parameterization of the heat and momentum transfer at high wind speeds are still not well understood and are difficult to measure, and thus they are the source of considerable uncertainty in hurricane models.

The ratio was kept at unity in all coupled experiments for lack of better knowledge.

5) TROPOAUSE TEMPERATURE

The Carnot theory of hurricanes (Emanuel 1988) predicts a strong sensitivity to the temperature in the outflow region, where heat is lost to space by radiation. The equivalent parameter in our model is the sum of the temperature differences between the top and bottom of each layer, that is, the total "temperature depth" of the model. The larger this temperature depth, the stronger the storm. Figure 5 shows the results of a set of

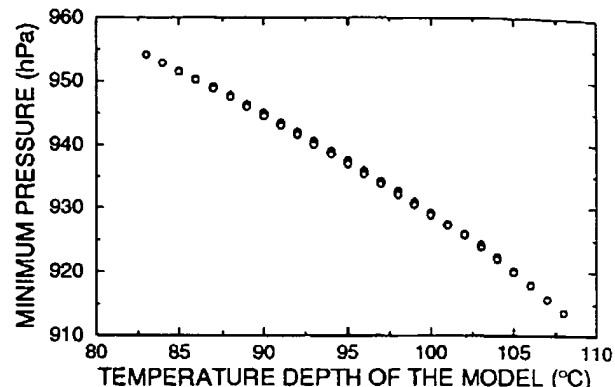


FIG. 5. Sensitivity of the steady-state central pressure to the total temperature depth of the model.

experiments around the default value of 95°C with a slope of a little less than -2 hPa/K .

c. Ocean model

The oceanic response to a moving hurricane has been investigated in great detail and even simple mixed layer models were found to reproduce the main characteristics of this response rather well (e.g., Price 1981, 1983; Price et al. 1994). Therefore the "Price-type" model due to Cooper and Thompson (1989) was chosen, as it has been tested carefully by the original authors and could be used without modifications for our purpose.

The ocean model is run with three active layers: a thin well-mixed layer on top of a strongly stratified layer and a deep abyssal layer. Momentum is turbulently exchanged at the interface with the atmosphere. In the interior of the ocean, vertical exchange of mass and heat is allowed only between the topmost layer representing the oceanic mixed layer and the next lower layer, called the upper thermocline. This exchange represents a turbulent mixing process referred to as entrainment. The Richardson number formulation of Price (1983) is used to parameterize the entrainment. This formulation effectively keeps a bulk Richardson number close to critical under wind forcing. The heat budget of the mixed layer is dominated by the entrainment heat flux through the base of the mixed layer. The exchange of heat between atmosphere and ocean is negligible by comparison (e.g., Bender et al. 1993) and is therefore not included in the model. Besides these turbulent processes gravity wave dynamics govern the ocean's behavior.

The horizontal resolution of the ocean model ranges from 10 to 25 km depending on the size of the hurricane as given by the size parameter η (see below for details). The time step depends on the chosen resolution and ranges from 5 to 12 min.

The characteristic features of the observed SST changes in the wake of tropical cyclones is reproduced by the model. A strong bias to the poleward side of the track can be seen with maximum SST reductions of

typically 2° – 6°C behind the storm. The SST reduction under the eye of the storm is much smaller with typical values between 0.5° and 1.5°C .

d. Coupling procedure

Coupling the two models effectively means specifying the exchange of information between the models. As already mentioned above, the turbulent exchange of heat and momentum is parameterized using the bulk aerodynamic drag formula with a wind speed-dependent drag coefficient. The surface pressure field sets up a barotropic flow within the ocean. This effect is neglected because the resulting flow is very weak and does not affect the entrainment process. Also neglected is the effect of the oceanic surface currents on the drag between atmosphere and ocean because the currents are extremely slow compared to the wind speeds in the atmosphere close to the surface. In contrast, the translation velocity of the hurricane relative to the ocean can reach a significant fraction of the wind speed 10 m above ground and therefore is included in the calculation of the turbulent exchange between the two models.

Additional complications arise from the different geometries of the models. Since the hurricane model is axisymmetric it does not "know" about horizontal directions other than radial distance from its central axis. Therefore the translation velocity at which the storm moves across the ocean must be specified externally. At the surface the radial nodes of the hurricane model are points in the radial direction and concentric circles in a horizontal plane. The SST felt by the hurricane model at a specific radial node therefore must be calculated as the average SST along a node circle. This amounts to an approximation that is reasonably close to the storm center where the rapid rotation causes rather effective homogenization along node circles. Far away from the storm center, this approximation must break down. Fortunately, the fractional part of anomalous SSTs along a node circle rapidly becomes smaller with increasing distance from the storm center such that the approximation becomes good again for large radii and, moreover, the storm intensity is not very sensitive to SST perturbations at large radii.

To construct the surface drag field for the ocean model the radial distance of each ocean grid point from the current storm center is calculated. The axisymmetric part of the surface wind field is then calculated by linear interpolation between the radial nodes of the hurricane model. Next, the vector sum of this axisymmetric wind and the prescribed storm translation velocity is calculated. The resulting total surface wind is finally used in the bulk aerodynamic drag formula to calculate the surface drag field felt by the ocean. An axisymmetric SST field for the hurricane model is calculated by bilinear interpolation from the nearest four ocean grid points to sampling points on the hurricane model's node circles. These sampling points are closely spaced where the

strongest SST gradients occur and far apart elsewhere. A distance-weighted average of the SST at the sampling points of a particular node circle is finally passed to the hurricane model as the SST at this particular node of the hurricane model.

In summary, the ocean model is forced by a 3D surface wind field constructed from the axisymmetric flow in the hurricane model and the hurricane translation velocity. In turn, the hurricane model is forced by an axisymmetric SST field constructed through azimuthal averaging of the 3D SST field of the ocean model around the storm center. The respective boundary fields are updated each time step.

As mentioned above, the steady-state hurricane is insensitive to the initial conditions in the hurricane model. In particular, the size of the steady-state hurricane cannot be set by the initial conditions. Since it is nevertheless desirable to force the ocean with storms of different sizes, a size parameter, η , was introduced in the coupling procedure. The atmospheric fields are remapped with a horizontal scale factor of η before they are passed to the ocean model. Analogously, the oceanic fields are remapped with a horizontal scale factor of η^{-1} before they are passed to the hurricane model.

4. Choice of parameters

Many parameters play a role in the SST feedback mechanism. Based on the sensitivity studies with the uncoupled hurricane model (section 3b) and on the results of earlier investigations of the oceanic response to hurricane forcing (e.g., Price 1983), a set of relevant parameters was selected.

- The steady-state hurricane intensity depends strongly on the environmental boundary layer relative humidity (H), on the SST, and on the tropopause temperature (T_{top}).
- The storm size (η) and the storm translation velocity (u_T) determine the interaction timescale between atmosphere and ocean.
- The thermal and dynamical inertia of the mixed layer is set by the unperturbed oceanic mixed layer depth (h_o).
- The stratification below the mixed layer ($\Gamma \equiv \partial T / \partial z$) affects both the availability of cooler water and the speed of the entrainment process.
- Last, the Coriolis parameter (f_o) sets the frequency of the inertial oscillations that dominate the oceanic wake. It also affects the amplitude of the vertical displacement of isopycnals as part of the inertio-gravity wave response. This displacement is larger at lower latitudes.

These eight parameters are considered to govern the SST feedback effect in the coupled model and thus define the parameter space to be explored.

Since it is very expensive to systematically sample an eight-dimensional parameter space it is desirable to

TABLE 1. Dimensional parameters.

Parameter	Dimension	Remarks
$D_1 \equiv h_o$	m	
$D_2 \equiv u_T$	$m s^{-1}$	
$D_3 \equiv \rho_o^{-1} \Delta p_{SST}$	$m^3 s^{-2}$	
$D_4 \equiv \eta L_o$	m	$\rho_o = 1.25 \text{ kg m}^{-3}$ is a reference density of air
$D_5 \equiv f_o$	s^{-1}	$L_o = 5 \times 10^4 \text{ m}$ is a scaling length
$D_6 \equiv \alpha \Gamma$	m^{-1}	
$D_7 \equiv 1 - \mathcal{H}$	l	$\alpha = 3.4 \times 10^{-4} \text{ }^{\circ}\text{C}^{-1}$ is the coefficient of thermal expansion

reduce the dimensions of the parameter space. This can be done if some of the parameters enter the problem under consideration only as a fixed combination. For example, \mathcal{H} , SST, and T_{top} enter the SST feedback by setting the storm intensity at constant SST (Δp_{SST}), that is, the intensity without SST feedback. Also \mathcal{H} determines the thermodynamic disequilibrium at the sea surface and thus the sensitivity to changes in SST. Therefore, the two-parameter set [Δp_{SST} , \mathcal{H}] can be used instead of the three-parameter set [\mathcal{H} , SST, T_{top}], reducing the dimension of the parameter space by one.

As it is not always as obvious as in the above example which combination of parameters is relevant to a given problem, the constraint of dimensional consistency can be used to transform a set of m parameters with physical dimensions into another set of $m-n$ nondimensional parameters. According to the Buckingham π theorem (Buckingham 1914) n is the number of independent physical dimensions of the m parameters.

Table 1 lists the suitably scaled dimensional parameters that are considered to govern the SST feedback effect. As only two physical dimensions are contained in this set of seven dimensional parameters [D_i] a set of five nondimensional parameters [N_i] can be defined that still spans the same phase space as the dimensional set [D_i]. There is no unique way of combining the dimensional parameters into nondimensional parameters. The following combination was chosen here:

$$\begin{aligned} N_1 &= D_4 D_1^{-1} = \eta L_o h_o^{-1} \\ N_2 &= D_3 D_2^{-2} = \Delta p_{SST} (\rho_o u_T^2)^{-1} \\ N_3 &= D_1 D_6 = h_o \alpha \Gamma \\ N_4 &= D_2 (D_4 D_5)^{-1} = u_T (\eta L_o f_o)^{-1} \\ N_5 &= D_7 = 1 - \mathcal{H}. \end{aligned} \quad (2)$$

TABLE 2. Explored dimensional parameter ranges.

Parameter	Range
h_o	$20 \text{ m} \leftrightarrow 80 \text{ m}$
u_T	$4 \text{ m s}^{-1} \leftrightarrow 10 \text{ m s}^{-1}$
Δp_{SST}	$37 \text{ hPa} \leftrightarrow 92 \text{ hPa}$
η	$0.4 \leftrightarrow 1.0$
f_o	$5 \times 10^{-5} \text{ s}^{-1}$
Γ	$0.08 \text{ }^{\circ}\text{C m}^{-1}$
\mathcal{H}	$78\% \leftrightarrow 87\%$

The SST feedback factor F_{SST} is an unknown function of the set of nondimensional parameters [N_i]. This function can be determined experimentally by sampling the five-dimensional parameter space defined by [N_i] with the coupled model. The sampled ranges of the dimensional parameters are listed in Table 2. The corresponding ranges of the nondimensional parameters are given in Table 3.

5. Results

A total of 2083 samples were taken in the region of the parameter space given in Table 3. "Taking a sample" here refers to integrating the coupled hurricane-ocean model for 18 days by which time the model had settled into a statistically steady state. Figure 1 shows the typical evolution of the surface pressure in the eye of the storm as a solid line. The dashed line displays the pressure time series in the control experiment, which differs only in one aspect: the SST is artificially held constant to exclude any SST feedback. Clearly, the noninteractive control storm develops to much greater intensity than the storm that interacts with the ocean. The strength of the SST feedback effect is measured by the feedback factor defined by (1). For the storm displayed in Fig. 1 the SST feedback factor is $F_{SST} = -46\%$.

An example of a two-dimensional cross section through the parameter space is given in Fig. 6. Here F_{SST} is displayed in a contour plot as a function of D_1 (h_o) and D_2 (u_T). The exact location of this section in dimensional coordinates is $D_3 = 5440 \text{ m}^2 \text{ s}^{-2}$, $D_4 = 40 \text{ km}$, $D_5 = 5 \times 10^{-5} \text{ s}^{-1}$, $D_6 = 2.7 \times 10^{-5} \text{ m}^{-1}$, and $D_7 = 0.19$. The qualitative dependence of F_{SST} on h_o and u_T is rather intuitive: fast-moving storms are less affected by the SST feedback effect, as are storms over deep oceanic mixed layers with high thermal and dynamical inertia. Surprising is the amplitude of the modelled feedback factors, which range from -10% to less

TABLE 3. Explored nondimensional parameter ranges.

Parameter	Range
N_1	$250 \leftrightarrow 2500$
N_2	$30 \leftrightarrow 460$
N_3	$5 \times 10^{-4} \leftrightarrow 2 \times 10^{-3}$
N_4	$1.6 \leftrightarrow 10$
N_5	$0.13 \leftrightarrow 0.22$

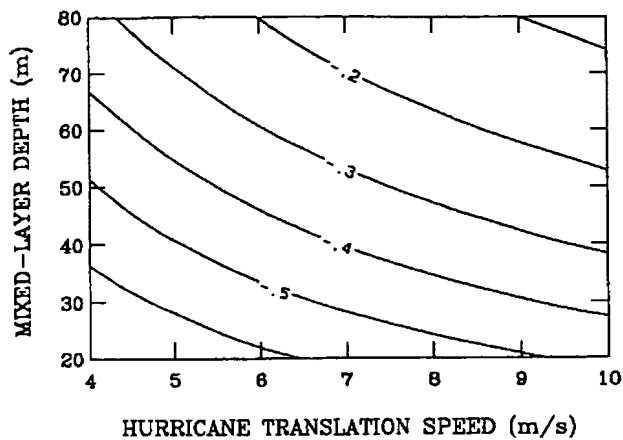


FIG. 6. The feedback factor F_{SST} as function of h_o and u_T . The contour interval is 10%. This cross section of the parameter space is taken at $\Delta p|_{\text{SST}} = 68 \text{ hPa}$, $\eta = 0.8$, $f_o = 5 \times 10^{-5} \text{ s}^{-1}$, $\Gamma = 0.08^\circ \text{C m}^{-1}$, and $\mathcal{H} = 81\%$.

than -60% . These numbers suggest that the SST feedback effect plays a key role in setting hurricane intensity. This in turn also means that subsurface oceanic features such as fronts or synoptic eddies have the potential to significantly affect hurricane intensity.

While Fig. 6 illustrates the dependence of the SST feedback factor on h_o and u_T for a particular choice of $(D_i)_{i=3,7}$ the overall dependence of F_{SST} on (D_i) [or on (N_i)] cannot easily be displayed graphically. Therefore an analytic approximation to the dependence of F_{SST} on (N_i) is sought. While only an approximation to the model results, an analytic expression is the most concise summary of the shape of F_{SST} in the phase space.

Inspection of the model results suggested a power law dependence of F_{SST} on (N_i) of the form

$$F_{\text{SST}}([N_i]_{i=1,5}) = \Phi(z), \quad (3)$$

with

$$z = e^{\lambda_0} \prod_{i=1}^5 N_i^{\lambda_i}, \quad (4)$$

where Φ is an unknown function and the exponents $[\lambda_i]_{i=0,5}$ are unknown coefficients. The set of 2083 samples of F_{SST} can now be used to determine the best-fit values of the unknowns. Let $\hat{\Phi}$ be the inverse of Φ . Then (4) can be written as

$$\ln[\hat{\Phi}(F_{\text{SST}})] = \lambda_0 + \sum_{i=1}^5 \lambda_i \ln(N_i), \quad (5)$$

which is linear in the unknowns $[\lambda_i]_{i=0,5}$. The function Φ cannot be optimized objectively without specifying a functional form. After detailed inspection of the data an exponential form was chosen:

$$\Phi(z) = \Phi_0 e^{-z}. \quad (6)$$

With these assumptions an iterative method can be used to determine the unknown parameters:

TABLE 4. Best-fit values of the regression coefficients.

Coefficient	Best-fit value
Φ_0	-0.87
λ_0	12.17
λ_1	-1.44
λ_2	-0.78
λ_3	-0.40
λ_4	-0.59
λ_5	0.46

- Step 1. Initial guess: $\Phi_0 = -1$.
- Step 2. Given Φ_0 , perform a multilinear least squares regression to yield $[\lambda_i]_{i=0,5}$.
- Step 3. Given values of $[\lambda_i]_{i=0,5}$ as result of step 2, perform a least squares regression to yield Φ_0 .
- Step 4. Go back to step 2 until Φ_0 does not change anymore between iterations.

This iterative method converges rapidly. The resulting best-fit values for the unknowns are listed in Table 4. Figure 7 displays the resulting analytic expression for F_{SST} as function of z together with all 2083 model runs. A histogram of the deviation of the fitted F_{SST} from the data is shown in Fig. 8; the standard deviation of the fitted F_{SST} from the data is $\sigma = 0.014$.

An analytic expression of the dependence of the SST feedback factor on the dimensional parameters $[D_i]_{i=1,7}$ can be obtained by use of Eqs. (2):

$$F_{\text{SST}} = -0.87 e^{-z}$$

with

$$z = .55 \left(\frac{h_o}{30 \text{ m}} \right)^{1.04} \left(\frac{u_T}{6 \text{ m s}^{-1}} \right)^{.97} \left(\frac{\Delta p|_{\text{SST}}}{50 \text{ hPa}} \right)^{-.78} \times \eta^{-.85} \left(\frac{f_o}{5 \times 10^{-5} \text{ s}^{-1}} \right)^{.59} \left(\frac{\Gamma}{8 \times 10^{-2}^\circ \text{C m}^{-1}} \right)^{-.40} \times \left(\frac{1 - \mathcal{H}}{.2} \right)^{.46}. \quad (7)$$

Reference values for the seven dimensional parameters have been used to formulate the equation in a physically meaningful form. If all the parameters are equal to their reference values the parameter z has a value of $z = 0.55$ and the SST feedback factor is $F_{\text{SST}} = -0.5$. Deviations from the reference values change the SST feedback factor in a physically intuitive way: a stronger negative feedback effect occurs when

- the oceanic mixed layer is thinner,
- the storm moves slower,
- the intensity potential is larger,
- the storm is of greater horizontal size,
- the storm occurs at lower latitudes,
- the thermal stratification below the oceanic mixed layer is stronger, and

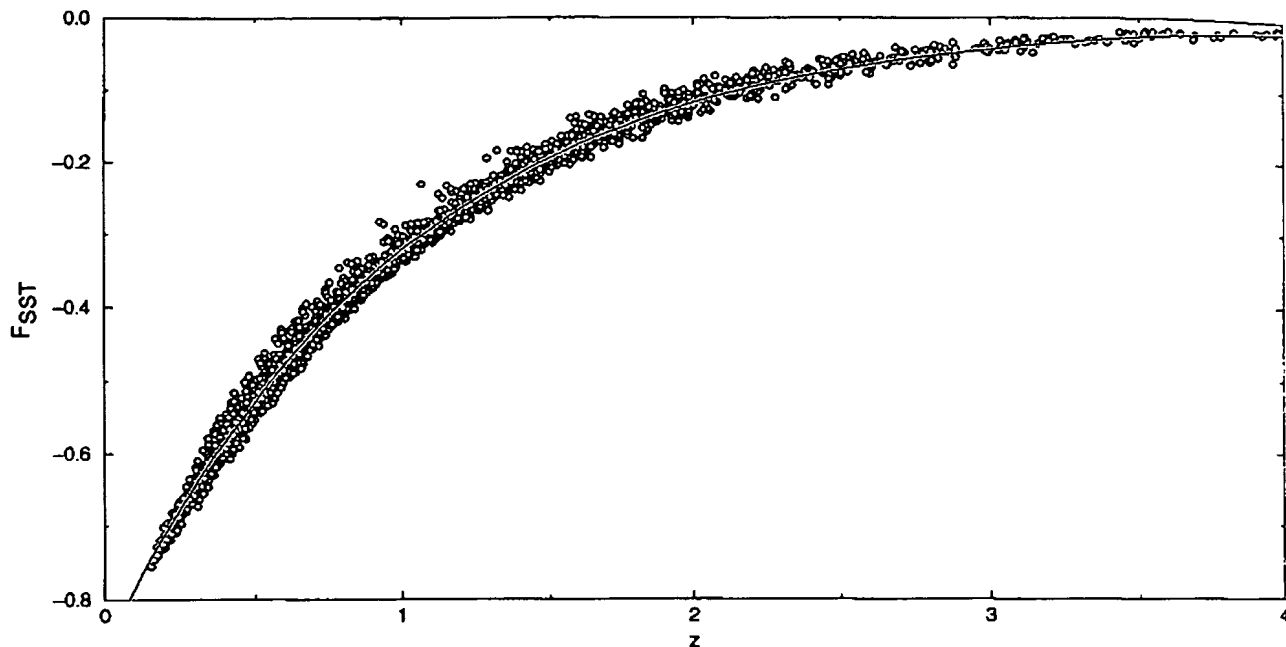


FIG. 7. The feedback factor F_{SST} as function of the parameter z for all model runs. The solid line is the best-fit function. Many of the 2083 data points are too close to the best fit line to be visible (see also Fig. 8).

- the relative humidity in the atmospheric boundary layer is higher.

Equation (7) is a very good approximation to the behavior of the coupled model in the explored region of the phase space as can be seen in Fig. 8. Its purpose is to summarize a rather complex physical process in a very concise fashion. Yet unlike the coupled model, the statistical regression is a purely mathematical tool. It does not know of the physics contained in the model equations. This is both its weakness and strength. It is weak because it cannot take advantage of the known laws of physics governing the problem and thus is valid strictly only in the sampled region of the phase space, and it is strong because it does not require knowledge

of all relevant physical processes but rather considers the overall effect of these processes. The approach taken here therefore consists of two very distinct steps. In the first step a simple model of the coupled hurricane-ocean system is constructed. This involves selecting a number of physical processes that are believed to be relevant to the problem and need to be represented adequately in the model. In the second step the output from the coupled model is treated as given and a concise mathematical description of the data is sought. This second step much resembles the analysis of observational data. A final third step in which the data is approximated with a simple physical model rather than with a statistical model is beyond the scope of this paper and is the subject of ongoing research.

6. Conclusions

Using a simple coupled hurricane-ocean model it was demonstrated that the interaction with the ocean significantly reduces the intensity of hurricanes. If the pressure deficit in the eye of the storm is taken as the intensity measure, the SST feedback effect can easily cut the intensity of a hurricane in half compared to a hypothetical storm over an ocean with constant SST. Unfortunately, observational data cannot be used to directly measure SST feedback factors because the necessary control storm over an ocean with constant SST does not exist.

Various environmental effects, such as that of background shear or of upper-tropospheric disturbances, are not included in the simple model. Similarly, the effect

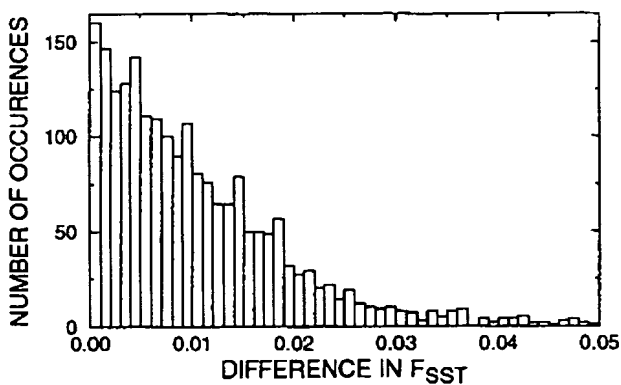


FIG. 8. Histogram of the difference between the modeled F_{SST} and the best-fit function.

of special oceanic situations associated with, for example, warm-core rings, the Gulf Stream, or shallow basins and shelf regions, is not considered in the simple model. The chosen modeling approach *assumes* that for the majority of storms these additional effects are small compared to the SST feedback effect. Conversely, it is expected that individual storms in atypical environments are not well described by the simple model. Regardless of the validity of this basic assumption, it should be kept in mind that the SST feedback is superimposed onto all other processes affecting hurricane intensity, because it directly affects the most fundamental process of a tropical cyclone, the transfer of heat from the ocean to the atmosphere.

Theories for the intensity of tropical cyclones (e.g., Emanuel 1986, 1995; Holland 1997) suggest that over much of the tropical ocean and throughout most of the hurricane season there is the potential for very intense hurricanes. Yet only few of the observed storms develop to the maximum intensity predicted by those theories. The recent revision of Emanuel's theory (Bister and Emanuel 1998), which accounts for the dissipative heating in hurricanes, leads to an even bigger gap between the actually attained intensity and the maximum possible intensity. The authors believe that the SST feedback effect can account for much of this discrepancy.

The model results presented in this paper cast a new light on the effect of the ocean on hurricane intensity. Besides the large-scale SST field, the synoptic-scale subsurface ocean conditions significantly affect a hurricane's intensity. A successful intensity forecast therefore requires knowledge of the upper-oceanic conditions ahead of the storm. Such information could be collected on a routine basis with aircraft expandable bathythermographs as part of hurricane reconnaissance flights.

It is hoped that more attention will be focused on the role of the ocean in limiting hurricane intensity. Much of the theory of turbulent transfer processes both in the ocean and at the interface between ocean and atmosphere is based on laboratory experiments and on the extrapolation to hurricane conditions of measurements taken at low or moderate wind speeds. In light of the fundamental role these transfer processes play in supplying energy to the hurricane, this aspect of the hurricane problem seems to be one of the most promising for major improvements in hurricane intensity forecasting.

Acknowledgments. This work was supported by the Office of Naval Research under Grant N00014-90-J-1101.

REFERENCES

- Bender, M. A., I. Ginis, and Y. Kurihara, 1993: Numerical simulations of tropical cyclone–ocean interaction with a high resolution coupled model. *J. Geophys. Res.*, **98**, 23 245–23 263.
- Bister, M., and K. A. Emanuel, 1998: Dissipative heating and hurricane intensity. *Meteor. Atmos. Phys.*, **65**, 233–240.
- Buckingham, E., 1914: On physically similar systems: Illustrations of the use of dimensional equations. *Phys. Rev.*, **4**, 345–376.
- Chang, S. W., and R. A. Anthes, 1979: The mutual response of the tropical cyclone and the ocean. *J. Phys. Oceanogr.*, **9**, 128–135.
- Cooper, C., and J. D. Thompson, 1989: Hurricane-generated currents on the outer continental shelf. Part 1: Model formulation and verification. *J. Geophys. Res.*, **94**, 12 513–12 539.
- Emanuel, K. A., 1985: An air-sea interaction theory for tropical cyclones. Part I. *J. Atmos. Sci.*, **42**, 1062–1071.
- , 1988: The maximum intensity of hurricanes. *J. Atmos. Sci.*, **45**, 1143–1155.
- , 1989: The finite amplitude nature of tropical cyclogenesis. *J. Atmos. Sci.*, **46**, 3431–3456.
- , 1995: Sensitivity of tropical cyclones to surface exchange coefficients and a revised steady-state model incorporating eye dynamics. *J. Atmos. Sci.*, **52**, 3969–3976.
- Foley, G. R., H. E. Willoughby, J. L. McBride, R. L. Elsberry, I. Ginis, and L. Chen, 1995: Global perspectives on tropical cyclones. WMO/TD-No. 693, Rep. TCP-38, 289 pp. [Available from the World Meteorological Organization Secretariat, 41 Av. Giuseppe Motta, Case Postale No. 2300, CH 1211 Geneva 2, Switzerland.]
- Holland, G. J., 1997: The maximum potential intensity of tropical cyclones. *J. Atmos. Sci.*, **54**, 2519–2541.
- Khain, A. P., and I. Ginis, 1991: The mutual response of a moving tropical cyclone and the ocean. *Beitr. Phys. Atmos.*, **64**, 125–141.
- Kleinschmidt, E., 1951: Grundlagen einer Theorie der tropischen Zyklonen. *Arch. Meteor. Geophys. Bioklimatol.*, **A4**, 53–72.
- Leipper, D. F., 1967: Observed ocean conditions and hurricane Hilda, 1964. *J. Atmos. Sci.*, **24**, 182–196.
- Ooyama, K., 1969: Numerical simulation of the life cycle of tropical cyclones. *J. Atmos. Sci.*, **26**, 3–40.
- , 1982: Conceptual evolution of the theory and modeling of the tropical cyclone. *J. Meteor. Soc. Japan*, **60**, 369–379.
- Price, J. F., 1981: Upper ocean response to a hurricane. *J. Phys. Oceanogr.*, **11**, 153–175.
- , 1983: Internal wave wake of a moving storm. Part I: Scales, energy budget, and observations. *J. Phys. Oceanogr.*, **13**, 949–965.
- , T. B. Sanford, and G. Z. Forristall, 1994: Forced stage response to a moving hurricane. *J. Phys. Oceanogr.*, **24**, 233–260.
- Riehl, H., 1950: A model for hurricane formation. *J. Appl. Phys.*, **21**, 917–925.
- Schade, L. R., 1994: The ocean's effect on hurricane intensity. Ph.D. dissertation, Massachusetts Institute of Technology, 127 pp.
- Sutyrin, G. G., and A. P. Khain, 1984: Effect of the ocean-atmosphere interaction on the intensity of a moving tropical cyclone. *Atmos. Oceanic Phys.*, **20**, 787–794.
- , —, and E. A. Agrenich, 1979: Interaction of the boundary layers of the ocean and atmosphere in a tropical cyclone. *Meteor. Gidrol.*, **2**, 45–56.
- Wu, C.-C., and K. A. Emanuel, 1993: Interaction of a baroclinic vortex with background shear: Application to hurricane movement. *J. Atmos. Sci.*, **50**, 62–76.

**This Page is Inserted by IFW Indexing and Scanning
Operations and is not part of the Official Record**

BEST AVAILABLE IMAGES

Defective images within this document are accurate representations of the original documents submitted by the applicant.

Defects in the images include but are not limited to the items checked:

- BLACK BORDERS**
- IMAGE CUT OFF AT TOP, BOTTOM OR SIDES**
- FADED TEXT OR DRAWING**
- BLURRED OR ILLEGIBLE TEXT OR DRAWING**
- SKEWED/SLANTED IMAGES**
- COLOR OR BLACK AND WHITE PHOTOGRAPHS**
- GRAY SCALE DOCUMENTS**
- LINES OR MARKS ON ORIGINAL DOCUMENT**
- REFERENCE(S) OR EXHIBIT(S) SUBMITTED ARE POOR QUALITY**
- OTHER:** _____

IMAGES ARE BEST AVAILABLE COPY.

As rescanning these documents will not correct the image problems checked, please do not report these problems to the IFW Image Problem Mailbox.